PNL-5218
UC-25

9D

Fabrication and Properties of Tungsten Heavy Metal Alloys Containing 30% to 90% Tungsten

W. E. Gurwell
R. G. Nelson
G. B. Dudder
N. C. Davis

September 1984

Prepared for the U.S. Department of Energy
under Contract DE-AC06-76RLO 1830

Pacific Northwest Laboratory
Operated for the U.S. Department of Energy
by Battelle Memorial Institute

Battelle

PNL-5218

DISCLAIMER

PACIFIC NORTHWEST LABORATORY
operated by
BATTELLE
for the
UNITED STATES DEPARTMENT OF ENERGY
under Contract DE-AC06-76RLO 1830

Printed in the United States of America
Available from
National Technical Information Service
United States Department of Commerce
5285 Port Royal Road
Springfield, Virginia 22161

NTIS Price Codes
Microfiche A01

Printed Copy

Pages	Price Cod
001-025	A02
026-050	A03
051-075	A04
076-100	A05
101-125	A06
126-150	A07
151-175	A08
176-200	A09
201-225	A010
226-250	A011
251-275	A012
276-300	A013

PNL-5218
UC-25

FABRICATION AND PROPERTIES OF TUNGSTEN HEAVY METAL ALLOYS CONTAINING 30% TO 90% TUNGSTEN

W. E. Gurwell
R. G. Nelson
G. B. Dudder
N. C. Davis

September 1984

Prepared for
the U.S. Department of Energy
under Contract DE-AC06-76RLO 1830

Pacific Northwest Laboratory
Richland, Washington 99352

ACKNOWLEDGMENTS

The following PNL staff made significant contributions to this work: K. V. Clark, J. E. Coleman, J. H. Hammer, D. J. Haverfield, H. E. Kissinger, R. T. Landsiedel, S. J. Morris, D. H. Parks, and C. B. Ruhter.

SUMMARY

In 1983, Pacific Northwest Laboratory conducted a survey of tungsten heavy metal alloys having lower-than-normal (<90%) tungsten content. The purpose of the work was to develop tougher, more impact-resistant high-density alloys for applications benefitting from improved mechanical properties.

Tungsten heavy metal alloys of 30% to 90% tungsten content were fabricated, and their mechanical properties were measured. Although ultimate strength was essentially independent of tungsten content, lower tungsten-content alloys had lower yield stress, hardness, and density, and decidedly higher elongations and impact energies. Cold work was effective in raising strength and hardness but detrimental to elongation and impact energies. Precipitation hardening and strain aging raised hardness effectively but had less influence on other mechanical properties.

CONTENTS

FIGURES

TABLES

INTRODUCTION

In 1983, Pacific Northwest Laboratory (PNL)[a] conducted a survey of tungsten heavy metal alloys having less-than-normal (<90%) tungsten content. The purpose of the work was to develop tougher, more impact-resistant high-density alloys for applications benefitting from improved mechanical properties. Most applications of tungsten heavy metal alloys require high density only (e.g., for radiation shielding and counterweights). Flywheels and boring bars are examples of applications for which performance would be enhanced by a stronger or tougher material that still retains a usefully high density.

Tungsten heavy metal alloys are true composites having a brittle, high-density, strain-rate-sensitive tungsten phase dispersed in a rather ductile matrix of moderate density that is less strain-rate sensitive. Generally, face-centered-cubic metals (such as the matrix phase of these W-Ni-Fe alloys) are less strongly affected by strain rate and temperature than body-centered-cubic metals (such as W) (Guy 1959). Also, contact points between individual tungsten particles are weak and are sources of crack initiation in well-sintered alloys; other investigators have observed and reported this phenomenon (Churn and German 1984; Churn and Yoon 1979; Lea, Muddle, and Edmonds 1983). The number and the effect of these weak tungsten-to-tungsten interfaces would decrease with decreased tungsten content. Therefore, improvements in mechanical properties, especially impact behavior, should be attainable by increasing the proportion of matrix phase relative to the tungsten phase. Commercially available alloys contain 90 to 98 wt% tungsten. This investigation covers tungsten heavy metal alloys containing 30% to 90% tungsten.

Liquid-phase (LP) sintering is the rule for commercially available tungsten heavy metals, because poor ductility is obtained from solid-state (SS) sintering of >90% tungsten compositions. However, in <90% tungsten compositions, good ductilities can be obtained from LP sintering. Both LP and SS

(a) Operated for the U.S. Department of Energy by Battelle Memorial Institute.

sintering, where applicable, were used in this work. In all cases the iron-nickel portion of the alloys was held constant by maintaining the nickel/iron ratio at 7/3.

The theoretical microstructure and density of 20% to 100% tungsten alloys were calculated. The Materials Department at PNL sintered, rolled, and annealed alloys of 30% to 90% tungsten. Strain aging and precipitation hardening heat treatments were developed for the 40% tungsten alloys. The resulting alloy sheets were characterized in terms of density, hardness, microstructure, and tensile and impact properties.

CONCLUSIONS AND RECOMMENDATIONS

This investigation produced the following conclusions:

- Impact toughness and tensile elongation are a direct function of volume fraction of the tough matrix phase. LP-sintered material is tougher and more ductile than SS-sintered material. The practical limit of LP sintering is near 80 wt%, below which gravity settling of the W spheroids occurs. When settling occurs, a layer of the tough matrix material remains on top, which might be used to advantage in some applications.
- Toughness increases from annealing are optimized at 1400 to 1425°C in the solid state. Much higher gains are available for highly worked material and SS-sintered material by annealing in the liquid phase, because of the low contiguity derived from LP-sintering.
- Annealed 40% W was precipitation hardened from HRC 12 to 25. The aged material is tough, strong, and isotropic. Similar effects can be obtained by cold working the material 10%. Very high strengths combined with useful toughness and ductility are possible at higher levels of cold work.
- Variable results were obtained from strain-aging heat treatments of cold worked 40% W. The results are inconclusive as to the possibility of strain aging of the matrix, at least in well-reduced and sintered material from powders of normal purity.
- Billets suitable for rolling into sheet can be sintered from low-density (~30% dense) green bodies not requiring large presses or binders. High-energy-rate formation (HERF) is applicable to 40% W. HERF billets of 80% to 90% W were too brittle to roll, suffering from poor billet geometry and the lack of oxide reduction.
- There are many possible options for significantly cutting production costs of rolled W alloy sheets that might make them more cost competitive with other materials.

Many options exist for increasing the toughness of high-density W alloys, and few were touched upon in this study. Factors influencing toughness have been summarized by German, Hanafee, and DiGiallonardo (1984). Some specific areas related to this study are recommended for further investigation:

- improved processing techniques such as finer W powder size, mechanical alloying, and optimized sintering and heat treating cycles.
- analysis of the lower limit of LP sintering ~80% W. Such a material, with a minimum of mechanical working, should have a very good combination of toughness, tensile properties, and density. Optionally, a product requiring a high degree of mechanical working might be LP annealed (resintered) to restore maximal ductility and toughness.
- detailed analysis of annealing changes in microstructure and chemistry of phases and interfaces. Annealing effects on toughness in both as-sintered and cold worked materials are not fully understood. Significant effects are expected due to impurities and their distribution, and to recrystallization and grain growth in the W phase particles.
- use of surface coatings, as shown by Zukas (1976), to both improve toughness and lower the ductile-to-brittle transition temperature. This option should be pursued where coatings could be applied.

Finally, low-cost fabrication methods need to be selectively developed to make W alloys more cost competitive with other materials and thereby increase the demand for the tough, high-density W alloys.

THEORETICAL DENSITIES AND MICROSTRUCTURES

In order to better understand the density trade-off with decreased tungsten content as well as the composite behavior of these materials, relationships can be calculated among alloy density, weight percent tungsten, and volume percent tungsten phase. These alloys are true composites, having a nearly pure tungsten phase dispersed in a nickel-iron-tungsten alloy matrix. Electron microprobe analyses have found that the tungsten phase is typically 99.7% W and 0.3% Ni + Fe, confirming the work of Dzykovich et al. (1965) and Pfeiler (1980). For the purposes of these calculations the tungsten phase is assumed to be 100% W with a density of 19.254 g/cm^3.

The matrix tungsten composition depends on the nickel/iron ratio as well as on heat treatment. The nickel/iron ratio used throughout this study was 7/3, a commonly chosen ratio that was also used by Green, Jones, and Pitkin (1954) in their original work on tungsten-nickel-iron alloys. The 7/3 ratio is at the minima of the iron-nickel binary phase diagram, and is also the position of maximal variability of tungsten solubility with temperature in the iron-nickel solid solution (Henig, Hofmann, and Petzow 1981). The matrix is therefore susceptible to precipitation-hardening heat treatments. The solubility of tungsten varies from 30% at 1400°C to 15% at 800°C. Typical commercial heavy metals that are heat treated at ~1100°C have 20% to 25% W in the matrix alloy.

The theoretical matrix density was calculated for 20%, 25%, and 30% W in 7Ni/3Fe-ratio solid solutions using lattice parameters, determined by Wehr (1962), that were confirmed by Agababova and Chaporova (1969) and Minakova et al. (1980). The following relationships were developed to calculate either alloy density, volume percent tungsten phase, or total weight percent tungsten, given any one of the three values and the solubility of tungsten in the matrix:

$$V = \frac{\rho_{wa} - \rho_m}{\rho_w - \rho_m}$$

$$P = \frac{\rho_w V + C \rho_m (1-V)}{\rho_w V + \rho_m (1-V)}$$

$$\rho_{wa} = \rho_w V + \rho_m (1-V)$$

$$V = \frac{P-C}{P-C + \frac{\rho_w (1-V)}{\rho_m}}$$

where V = volume fraction W phase
P = weight fraction W in the alloy
ρ_{wa} = alloy density
C = weight fraction W in the matrix
ρ_w = W density, 19.254 g/cm^3
ρ_m = matrix density, 9.627 g/cm^3 with 20% W in solid solution
9.972 g/cm^3 with 25% W in solid solution
10.349 g/cm^3 with 30% W in solid solution.

The results for a solid solubility of 25% W are presented in Table 1. For comparison, the values for 20% and 30% solubility are also given at 30 wt% W. The density and vol% W do not vary much with W solubility, and this variance decreases as the matrix volume decreases (and as the tungsten content increases). The values in Table 1 agree well with the sintered densities achieved in 75% to 97% W by Green, Pitkin, and Jones (1954). The values in Table 1 are for fully dense, nonporous material.

There are two other useful relationships that have, however, more limited applications. The first relates V, P, and ρ_{wa}; given two of these and an assumed C and ρ_w = 19.254 g/cm^3, the remaining value can be calculated:

$$V = \frac{\rho_{wa} (P-C)}{\rho_w (1-C)} .$$

The second formula,

$$\frac{1}{\text{Sintered } \rho_{wa} + 0.05} = \frac{\% \text{ W}}{19.3} + \frac{\% \text{ Ni}}{8.9} = \frac{\% \text{ Fe}}{7.86}$$

seems crude, but it does produce surprisingly accurate alloy density values for a given tungsten content. For example, the calculated sintered density for a 40% W alloy is 10.96 g/cm^3, which compares very well with the 11.04 g/cm^3 value given in Table 1.

TABLE 1. Relationships Among Total Tungsten Content, Alloy Density, and Volume of Tungsten Phase. Based on matrix W content of 25 wt%, except where noted.

wt % Tungsten, W_w	Alloy Density, ρ_{wa}, g/cm^3	vol % Tungsten, V_w
20	9.63	0
25	9.97	0
30	10.30	3.6
30	10.27(a)	6.7(a)
30	10.35(b)	0(b)
40	11.04	11.5
50	11.88	20.6
60	12.87	31.2
70	14.03	43.7
80	15.43	58.8
85	16.23	67.4
90	17.13	77.1
91	17.32	79.2
95	18.13	87.9
100	19.254	100.0

(a) Matrix tungsten content of 20 wt%.
(b) Matrix tungsten content of 30 wt%.

SHEET FABRICATION

In order for the results of this work to be comparable with other heavy metal work, materials and procedures used by other investigators were also used here whenever possible. In particular, procedures given by Myhre (1979) were found to be useful.

POWDER CHARACTERISTICS AND PREPARATION

Commercially available tungsten, nickel, and iron powders were purchased in two lots each. The individual powder lots were essentially identical in the cases of tungsten and nickel, as shown in Table 2; lot analysis was not available for the small quantities of iron powder purchased for this work. The powder characteristics are typical of those used by other investigators (Lux et al. 1982; Myhre 1979; Henig, Hofmann, and Petzow 1981).

All powders were rescreened before blending to remove any agglomerates that formed during shipping and storage. Tungsten was screened through a 200-mesh sieve, and iron and nickel through a 325-mesh sieve. The weighed powder mixtures were mixed in a twin-shell blender for 30 min, with the intensifier bar running 1 min out of every 5 min. The iron/nickel ratio was held constant at 7/3 by weight in all blender charges. Charges were always chosen to fill the blender to working capacity for maximal blending and intensifier bar efficiency: 4 kg for 30% and 40% W blends, 5 kg for 70% W blends, and 6 kg for 80%, 85%, and 90% W blends.

The blended powders were fabricated into rolling billets by either of two methods: 1) tamping into ceramic boats and sintering, or 2) High-Energy-Rate Forming (HERF) compaction and diffusion annealing. In neither case were any additives used for any purpose such as lubricating or binding the powders; hence, there are no unwanted or unexpected binder effects on the mechanical properties of the resultant materials.

SINTERED BILLETS

Sintering experiments were conducted with 40% W powder to establish the preparation techniques for all of the sintered billets. All sintering was done

TABLE 2. Powder Characteristics

Powder	%W	%Ni	%Fe	C, ppm	O, ppm	N, ppm	S, ppm	Average Particle Diameter,[a] µm	Apparent Density,[b] g/cm^3
Teledyne Wah Chang	99.95 typical	<0.002	<0.005	19	195			4.78	3.42
Type C-10 W[c]	99.9 minimum	<0.002	<0.005	15	180			4.2	3.19
INCO		<99.7	0.0002	650	500		2	4.37	2.00
Type 123 Ni			<0.0001	650	610		1	4.07	1.93
GAF	Typicals-no		>99.5	<1000	<3000	<1000		6 to 8	
Type HP Fe	lot analysis								2.2 to 3.2

(a) Fisher Sub-Sieve Sizer (F.S.S.S.); refer to ASTM B330.
(b) Scott Volumeter; refer to ASTM B329.
(c) <50 ppm Mo, Fe
<20 ppm Cr, Cu, Si, Ni
<10 ppm Al, Ca, Co, Mg, Mn, Na, Pb, Sn, Ti.

in a cold wall furnace using bottled argon and hydrogen without any purification or drying. Initial experiments were run with various gas mixtures ranging from 50% to 100% H_2; no significant differences in sintering behavior were found. Consequently, all subsequent sintering was done in 50% H_2/50% Ar.

Initially, powders were either compacted in steel dies at various pressures or merely tamped into small aluminum oxide crucibles or trays and then sintered in hydrogen/argon on high-purity aluminum oxide powder. Although the green density could be improved by increased compacting pressure, the sintered densities were much less sensitive to compacting pressure, as shown in Figure 1. For example, during SS sintering for 3 h at 1400°C, a compact pressed at 40 ksi (40,000 psi) sintered from 66% to 94% of theoretical density, and powder merely tapped down in a crucible sintered from 45% to 89% dense.

During LP sintering at 1500°C for 1 h, both low- and high-density green compacts sintered to full theoretical density. However, LP-sintered 40% W

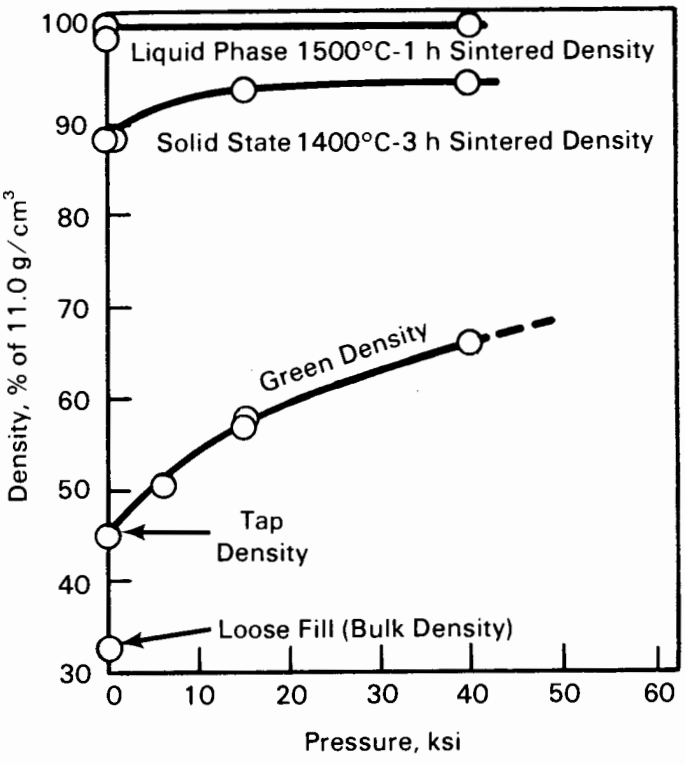

FIGURE 1. Density Versus Compacting Pressure for 40W-42Ni-18Fe

compacts were found to suffer from two problems: 1) high fluidity resulting in poor shape retention and 2) segregation due to gravity settling of the tungsten spheroids. These effects are illustrated in Figure 2. Salyer and O'Neil (1964) found that tungsten segregation occurred in compositions of less than 80% W (equal to approximately 60 vol% W) during sintering at 1460°C for 1 h. Green, Jones, and Pitkin (1954) did not note the occurrence of tungsten segregation in 75% W that was sintered for 1 h at 1440°C, a temperature which, they observed, "approximately coincides with the appearance of the liquid phase." Both investigations maintained the iron/nickel ratio at 7/3.

The results of our attempts to LP sinter 70% and 80% W are shown in Figure 3. It appears that very strict control of part geometry and melt viscosity (by maintaining the sintering temperature very close to the melting point) would be required to avoid segregation in compositions of 80% W and lower. To avoid segregated materials, SS sintering was performed throughout this study, and only the 85% and 90% W compositions were additionally LP sintered. However, the layer of matrix left at the top of segregated billets might be used in some applications to improve ductility and toughness in the manner of Zukas (1976), who improved the ductility of 90% W with diffusion coatings of Cu, Co, Ni, and Au. Zukas' work also showed that the ductile-to-brittle transition temperature (DBTT) was lowered by the coating. Notches are known to raise the DBTT (Dieter 1961), which suggests that the coatings nullify the "notches" that exist between tungsten particles at the surface of uncoated W heavy metal.

An interesting precipitated phase was found in the W spheroid-free areas that were depicted in Figures 2 and 3. This phase is illustrated in Figure 4. It is lamellar and has the appearance of pearlite. These structures were observed by Winkler and Vogel (1932), Takeuchi (1967), and Agababova and Chaporova (1969). Bukatov, Romashov, and Gostev (1983) produced a similar tungsten precipitate between W spheroids in specimens quenched from a sintering temperature of 1550°C. Henig, Hofmann, and Petzow (1981) identified similar W precipitates, which appeared after annealing for a few hours at 850°C; at very long times (~500 h), the lamellar W was replaced by discrete, rounded (Fe,Ni)W particles. The lamellar phase encountered in this study was too small to

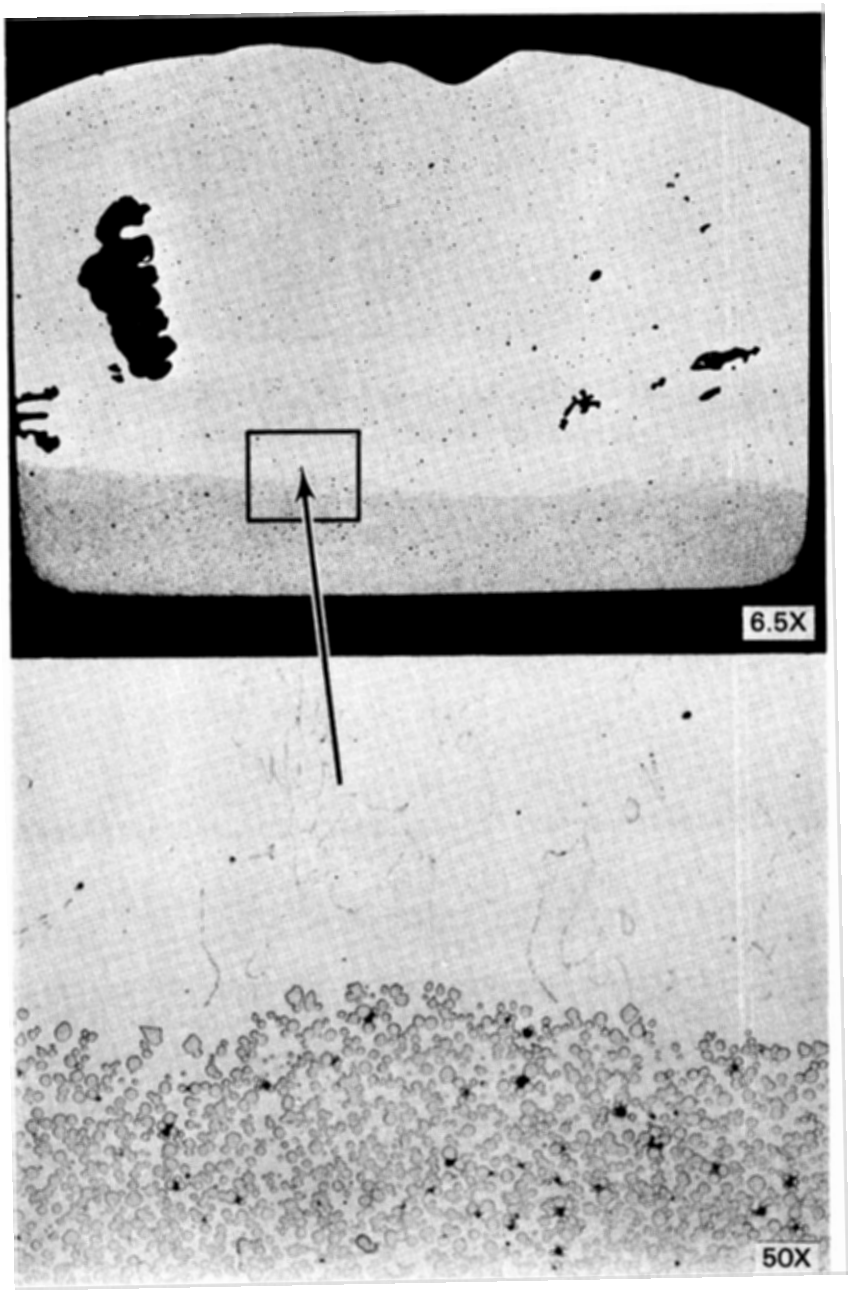

FIGURE 2. Tungsten Segregation in Liquid-Phase Sintered 40% W Pellet Pressed at 40 ksi and Sintered at 1500°C for 1 h. Slumped--assumed shape of crucible that contained it. Bottom layer: tungsten spheroids, gravity settled during sintering in Ni-Fe-W matrix. Top layer: basically Ni-Fe-W matrix with tungsten precipitates that were laid down during solidification.

a) 70% W Sintered 1 h at 1475°C
101.0% of 14.03 g/cm^3 (6.65X)

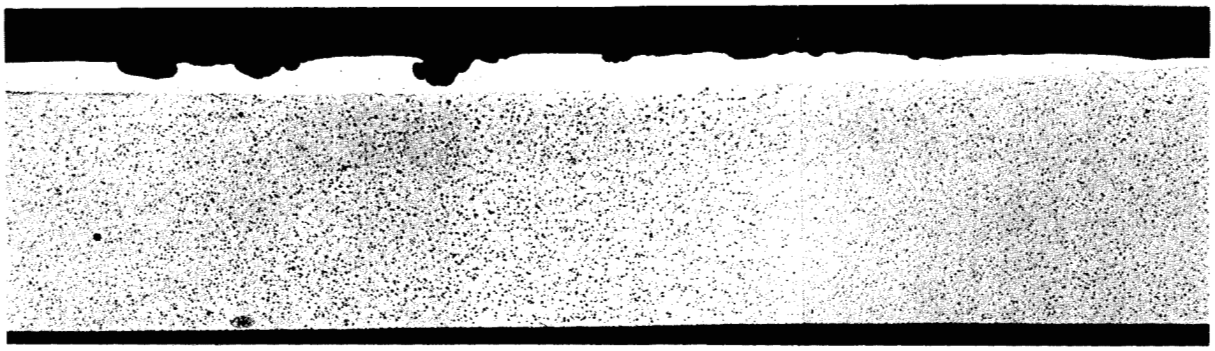

b) 80% W Sintered 1 h at 1470°C
98.1% of 15.43 g/cm^3 (8X)

FIGURE 3. Tungsten Segregation in 70% and 80% W. In 80% W sample a pool of molten matrix gathered in a low spot on the billet surface.

identify by energy dispersive x-ray analysis (EDAX), but was assumed to be W. Also, x-ray diffraction detected only bcc W and fcc γ(Ni-F-W) matrix.

Because the sintering results were so satisfactory for loosely tamped powders, it was decided to use the tamping technique to fabricate all the sintered billets used in this study. This decision was encouraged by the fact that available press capacity was limited and that no dies were available for making the large-area pressings needed for rolling billets. However, experience has proven that the technique used in laying up tamped beds of dry powder is critical to producing crack-free sintered billets. The technique must produce a crack-free green billet of uniform density (sharp steps in density, from step

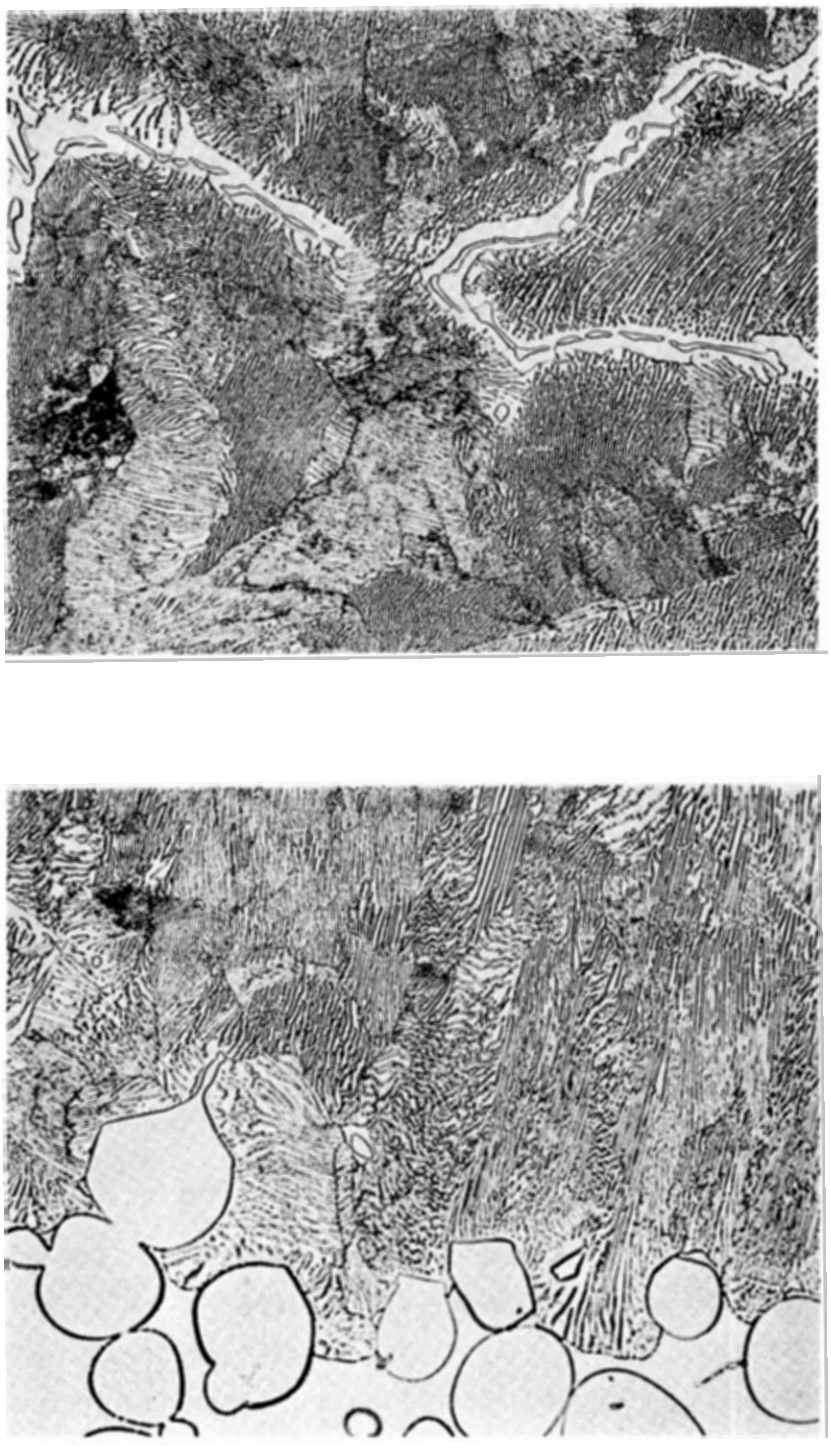

FIGURE 4. Lamellar Tungsten Precipitates Found in Areas Free of W Spheroids (see Figures 2 and 3). Etched, 500X.

tamping, introduced cracks in the sintered billet). Presumably, the much higher shrinkage experienced by the low-density green volumes is restrained by the higher-density volumes leading to cracking in the weakest planes of the low-density material. About 70% of tamped powder beds made by this technique sintered to crack-free billets. The others were discarded. It was assumed that any invisible internal cracks would be healed and obliterated by the subsequent rolling and annealing. The results of the mechanical property tests and metallography supported this assumption.

The containers for the tamped powder beds were commercially available 99.8% aluminum oxide trays that are made by slip-casting and sintering to high density. They are fine-grained and have a relatively smooth surface. The tray is 5 in. by 7 in. by 2 in. deep. The best technique found for laying up the powder bed in the tray was as follows:

- Use as blended powder with a minimum of agglomerated or otherwise compacted powder.
- Uniformly place (e.g., spoon) the powder to the thickness desired.
- Screed lightly to level. Never push a large amount of powder ahead of the screed. Leave excess powder at the end of the screed rather than trying to redistribute it evenly over the entire powder bed.
- Optionally, press lightly with a flat plate that covers the entire area screeded.
- Do not jar the powder mass.
- Sinter with slow heatup to obtain uniform sintering.

Green densities of these tamped powders were 30% to 40% of theoretical. Well-sintered billets were ~98% dense after either LP or SS sintering, as shown in Table 3. Typical sintered billet size, as illustrated in Figure 5, was 3.5 x 5.0 x 0.5 in. thick. Subsequent rolling and annealing increased the densities of all billets to 100%.

Success with the sintered billet fabrication techniques described above encouraged some attempts to fabricate large-area sheets that would then require

TABLE 3. Sintered Billets

Billet Number[a]	Reduction °C	Reduction Hours	Sinter °C	Sinter Hours	Sintered Billet Density,[b] g/cm³	Density After Rolling to 0.1-in.-Thick Sheet,[c] g/cm³	Theoretical Density,[d] g/cm³
30-2	900	1	1406	5	9.35	10.29	10.30
40-12	870	1.5	1425	3	9.75	11.00	11.04
13	890	1	1427	6	10.63		11.04
17	890	1	1412	5	10.41	10.98	11.04
70-4	900	1	1435	20	13.99	13.93	14.03
80-1	900	2	1430	16	15.32	15.33	15.43
-3	900	2	1427	20	15.28	15.36	15.43
85-2 (LP)	1100	2	1490	1	15.92	16.43	16.23
-4	1100	2.5	1430	18	16.01	16.13	16.23
90-10 (LP)	1100	2	1490	1	16.79	16.81	17.13
90-12	1100	2.5	1430	18	16.88	17.01	17.13

(a) First two digits of billet number are tungsten composition in weight percent. Next two digits are sequential billet number. (LP) = Liquid-phase sintered; all others SS sintered.
(b)ASTM B311, modified for large billets.
(c)ASTM B311.
(d)Theoretical densities from Table 1, based on 25% tungsten content in matrix.

little or no rolling. Although limited success was achieved, the results identified some possible avenues for future development of directly sintered sheets. This work is discussed in Appendix A.

ROLLING SINTERED BILLETS

All rolling of sheet was done on a 14-in. mill. Initial rolling of low-density 40% W billets showed that the billets densified during both cold rolling and annealing. Figure 6 shows the density of two billets as a function of rolling thickness reduction and time at 1400°C. These billets were sintered at 1400°C, as were all the subsequent intermediate anneals. From the data in Figure 6 it is possible to estimate the total thickness reduction and number of anneals required to reach 100% density. For instance, a 98%-dense sintered billet would require approximately 30% thickness reduction and one anneal to reach 100% density. As shown in Figure 7, billet hardness increases significantly with density, and is therefore a good indicator of density when the billet is annealed to a standard condition.

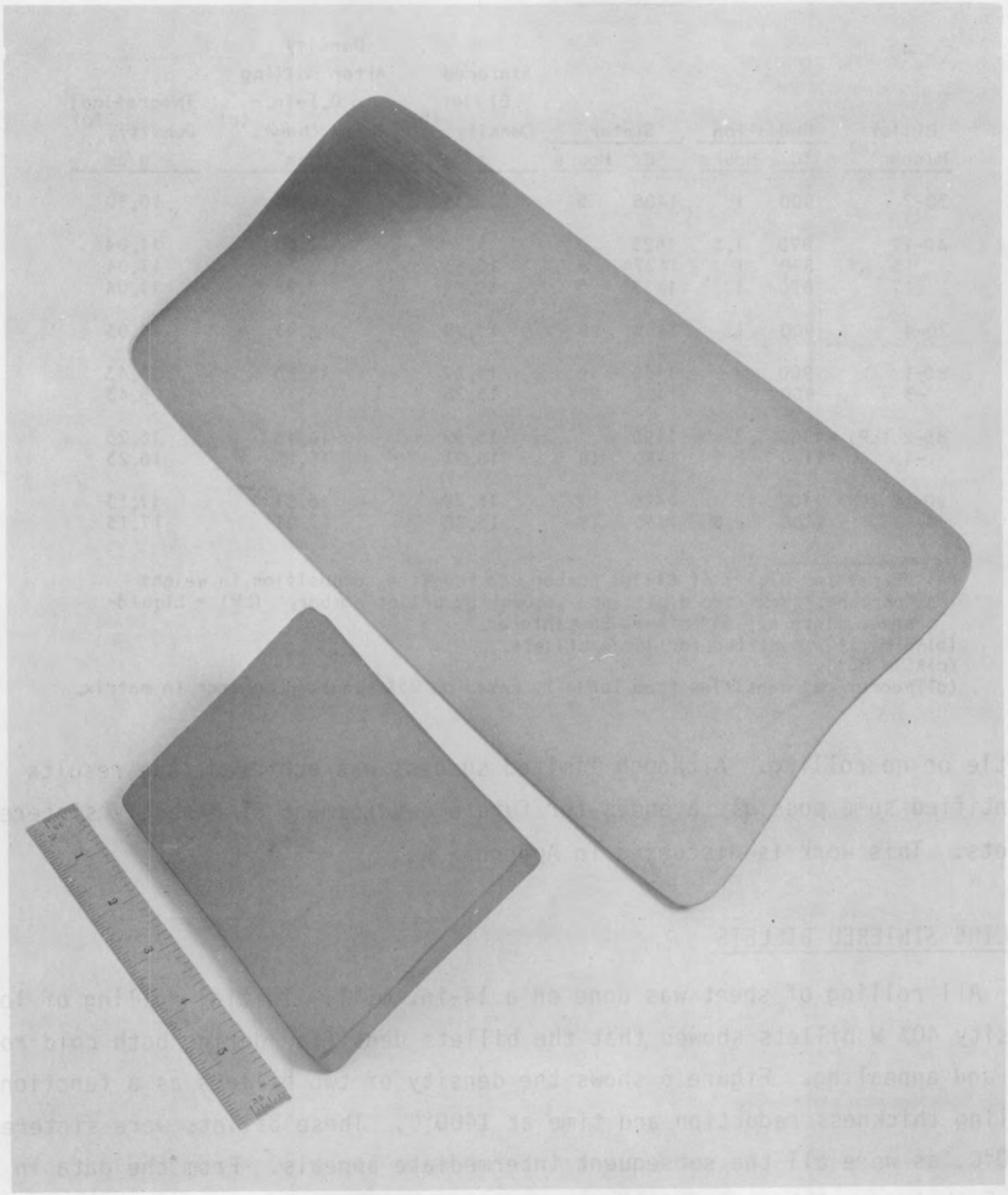

FIGURE 5. Typical Sintered Billet. Lower: as-sintered; upper: rolled to 0.1-in. thick.

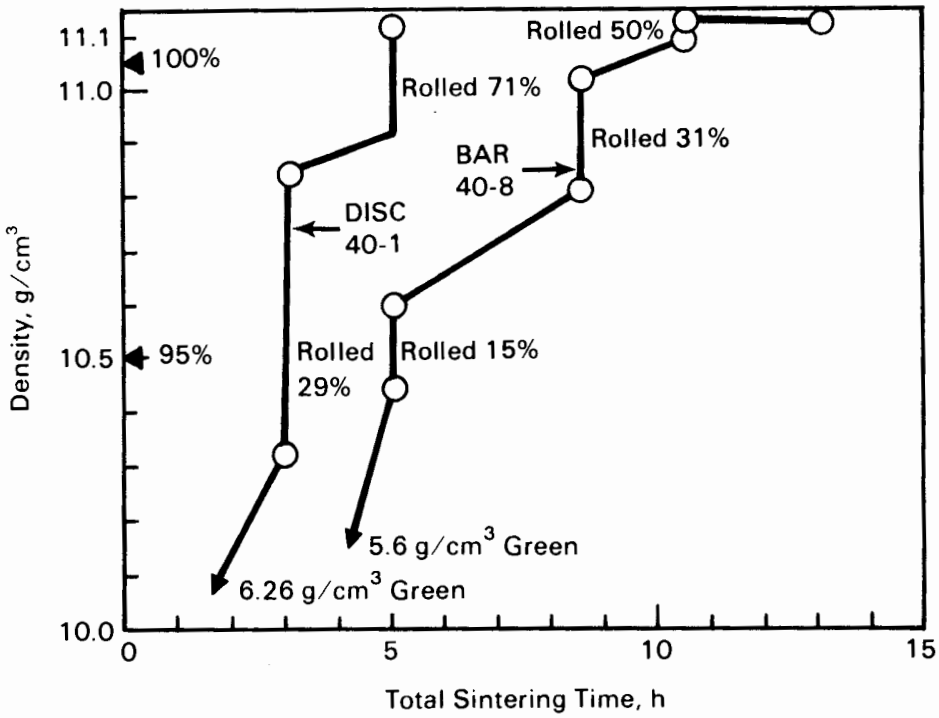

FIGURE 6. Density of 40% W as a Function of Total Sintering and Annealing Time at 1400°C and Rolling Reduction at Room Temperature

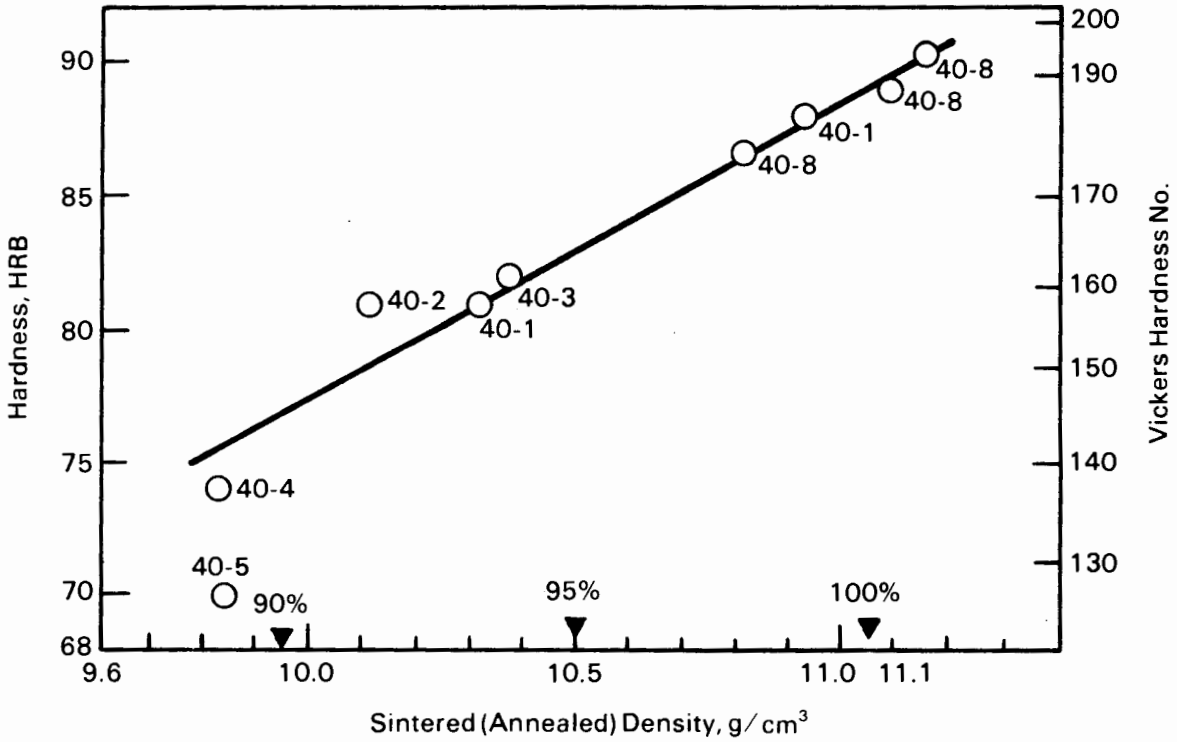

FIGURE 7. Annealed Hardness of 40% W as a Function of Density. Data points from billet numbers indicated.

All of these alloys in the range from 30% to 91% W work-harden rapidly as a function of rolling reduction, as shown in Figure 8. This behavior has long been recognized (Kershaw 1964; Krock and Shepard 1963); in fact, the ductility of W-Ni-Fe composites is attributable to the rapid work-hardening of the matrix phase, which is responsible for maintaining a sufficiently high hydrostatic stress field around the tungsten particles to cause deformation of the tungsten particles by slip rather than by fracture. As a practical matter, the rapid work-hardening of these alloy allows them to be strengthened appreciably while retaining useable levels of ductility.

In Figure 8 the 30%, 40%, 70%, and 80% W specimens were all SS sintered and rolled to a thickness of 0.1 in. The 85% and 91% W specimens were commercially available LP-sintered sheet, 0.1-in. and 0.06-in. thick, respectively. All specimens were given the same anneal at 1415°C for 5 h before the work-hardening experiment. All of the specimens elongated 60% or more during the cold rolling, indicating that the annealing conditions restored adequate ductility to these previously rolled sheet materials. Such high elongations were not attainable in the earlier stages of rolling because edge cracking occurs more easily in thicker material. The rolls provide increasing edge restraint as the sheet becomes thinner. Also, the as-sintered billets are mechanically weaker because of their lower densities.

The most frequently encountered rolling defect was edge cracking. In fact, the maximal reduction between anneals was usually determined by the onset of edge cracking. To continue beyond that point is to risk having a crack propagate halfway through the billet during a single pass through the rolls. Edge cracking was minimized by the following methods:

- All fine edge cracks were removed between anneals, preferably by processes that left a notch-free edge with a minimal amount of cold work. Wet abrasive cut-off sawing or wet belt sand were preferred. Preferably all billet conditioning was done before annealing.
- Large reductions ~10% per pass were made in order to work the entire thickness over the entire area of the billet. This helped prevent lamellar cracking, which is caused by elongating the surfaces more than the center of the billet. Also, the reduction

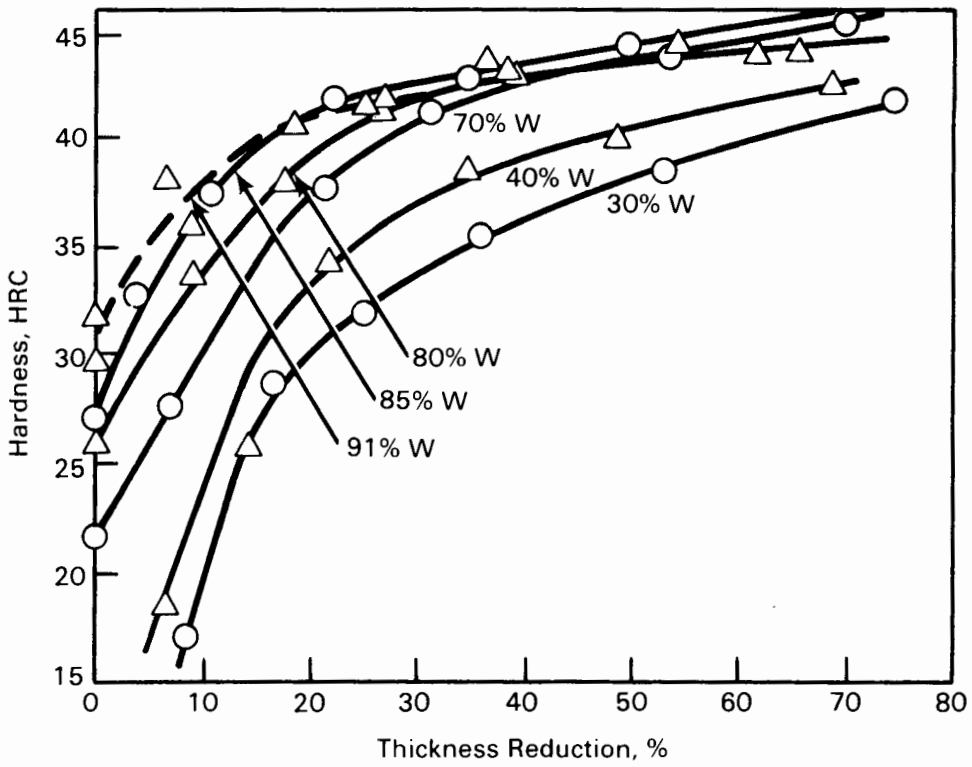

FIGURE 8. Hardness of Tungsten Alloys as a Function of Rolling Reduction at Room Temperature. Previously annealed at 1415°C for 5 h.

during the first roll pass on an as-sintered billet needs to be large enough to work the entire area of the billet. As-sintered billets contained thin spots that would tend to crack if the roll pass was not deep enough to apply a compressive stress to that area.

- Both edge and lamellar cracking tendencies were reduced by preheating the material to 500°C before rolling. The HERF billets tended to crack more frequently than the sintered billets. It was found that these billets rolled best at 500°C. Subsequently, all billets, whether sintered or HERF, were rolled at 500°C. All materials for which mechanical properties were measured were rolled at 500°C.

In general, the lower tungsten compositions rolled more easily, and the LP-sintered billets rolled more easily than the SS-sintered billets of the same composition. Typical microstructures for the alloys prepared in this study are shown in Figures 9 through 11. Figure 9 illustrates the differences in microstructure between LP- and SS-sintered materials. LP sintering produces a

spherical W phase of minimal surface area that allows the ductile matrix to form a more robust, continuous skeleton than that of the SS-sintered material. Much larger initial rolling reductions, about 30% to 40%, were possible with LP-sintered material. The 85% W SS-sintered billet cracked slightly after a 23% reduction and the 90% W billet cracked severely after only 13% reduction. However, after the first intermediate anneal the SS-sintered billets rolled to nearly twice the initial reduction before small edge cracks occurred; thereafter, their rolling behavior was very close to that of the LP-sintered billets. In fact, the microstructure of the SS-sintered billets is refined during repeated rolling and annealing as shown in Figure 9. After rolling and annealing several times, the microstructure of the SS-sintered material is similar to that of the LP-sintered billet.

The extent of SS-sintering was important for the higher tungsten compositions. A 70% W billet sintered at 1400°C for 4 h rolled poorly. After resintering at 1435°C for 20 h the material rolled more easily. The improved rolling performance could be predicted from the microstructural refinement and densification obtained from the higher temperature and longer time (see Figure 10).

HIGH-ENERGY-RATE FORMED BILLETS

Two separate groups of billets were HERF compacted to high density and then diffusion heat treated before rolling. The first group of billets was made from materials that had been in the laboratory for several years, and no chemical analyses were available. Their approximate particle size was estimated from the mesh size indicated on the labels. Billets made from this material are identified as 1C, 2C, 3F, and 4E, as shown in Table 4. In this group copper was substituted for nickel in billets 1C and 2C. To maintain the same density as the nickel-containing billets (11.1 g/cm^3), the composition was shifted from 40W-42Ni-18Fe to 36W-45Ni-19Cu.

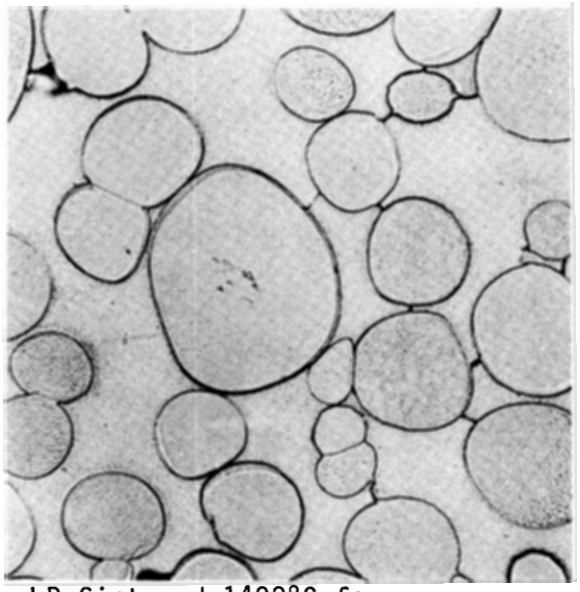

As-LP-Sintered 1490°C for
45 min. Hardness HRC 24

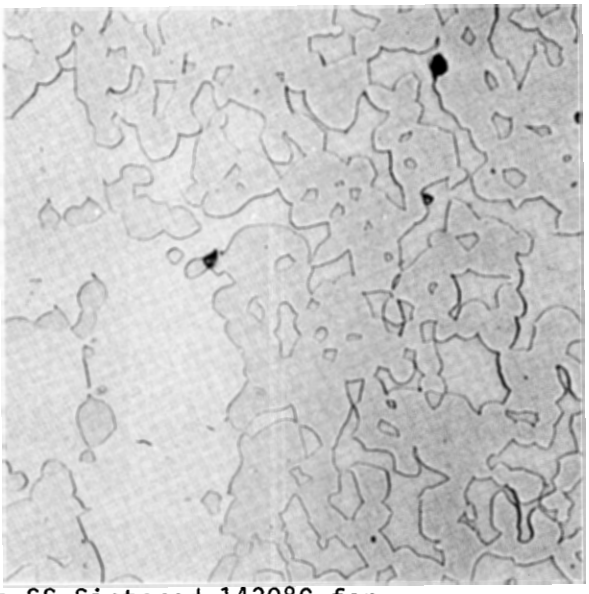

As-SS-Sintered 1430°C for
20 h. Hardness HRC 23

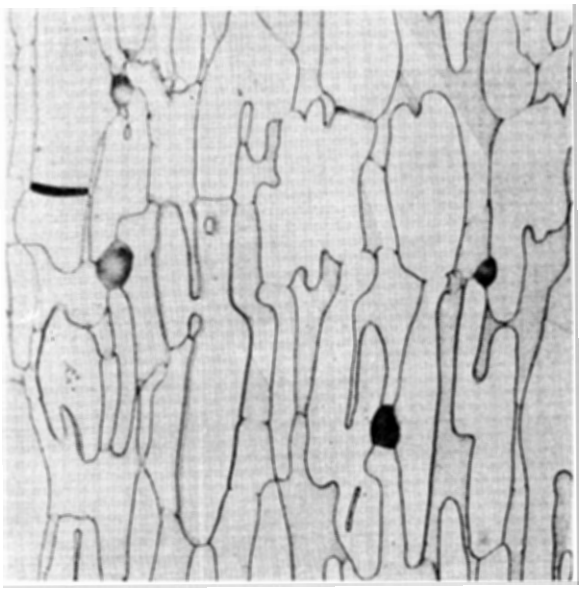

LP Sintered, Rolled to 0.1-in.
Thick, Annealed 1400°C for
21 h. Hardness HRC 26

SS Sintered, Rolled to 0.1-in.
Thick, Annealed 1400°C for
16 h. Hardness HRC 29

FIGURE 9. Typical Microstructures of 85% W. Transverse at 500X. Marked differences in as-sintered microstructures decrease with rolling and annealing.

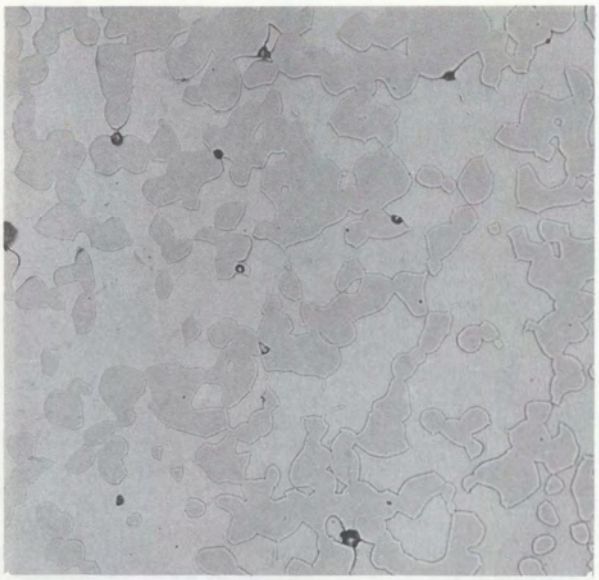

As-Sintered at 1435°C for 20 h--
14.0 g/cm^3. Hardness HRC 22

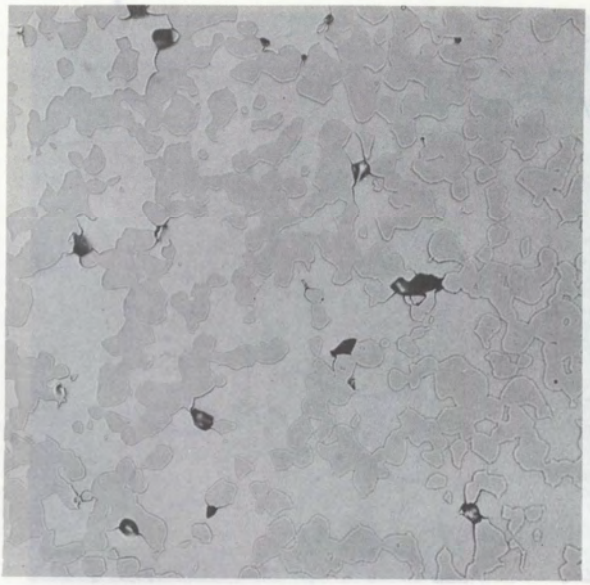

As-Sintered at 1400°C for 4 h--
13.5 g/cm^3. Hardness HRC 10

Sintered at 1435°C for 20 h, Rolled to
0.1-in. Thick and Annealed at 1400°C for
16 h. Hardness HRC 20

FIGURE 10. Microstructures of Solid-State Sintered 70% W. Transverse 500X. Higher sintering temperature and longer time coarsens and refines W particles and increases density, resulting in markedly better rolling performance.

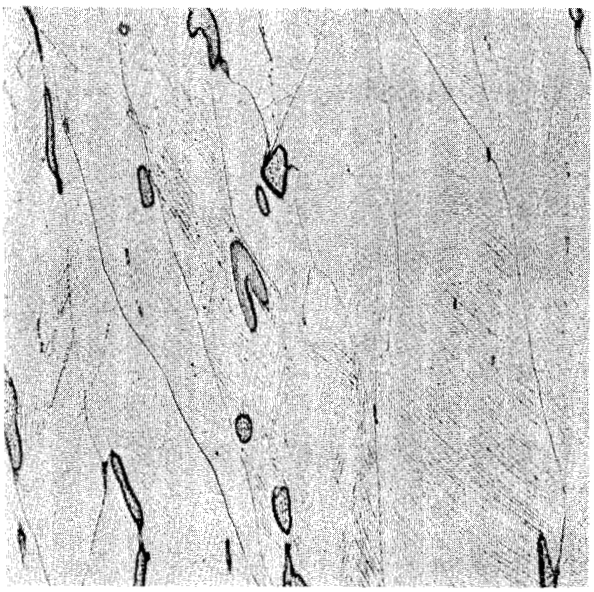

30% W As-Rolled 46%.
Hardness HRC 37

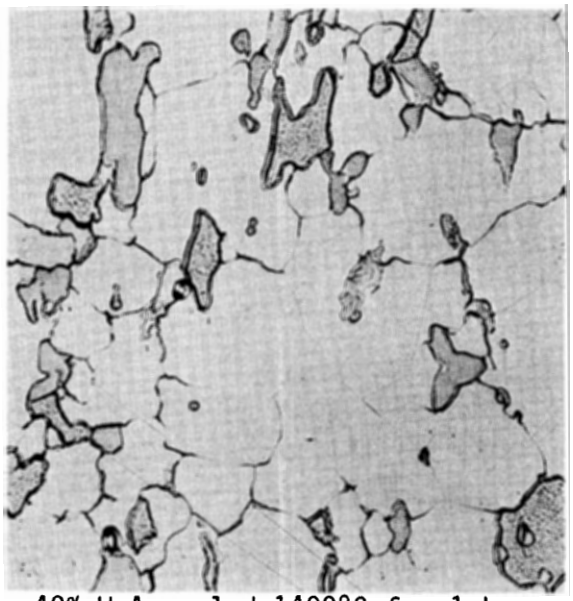

40% W Annealed 1400°C for 1 h.
Hardness HRC 12

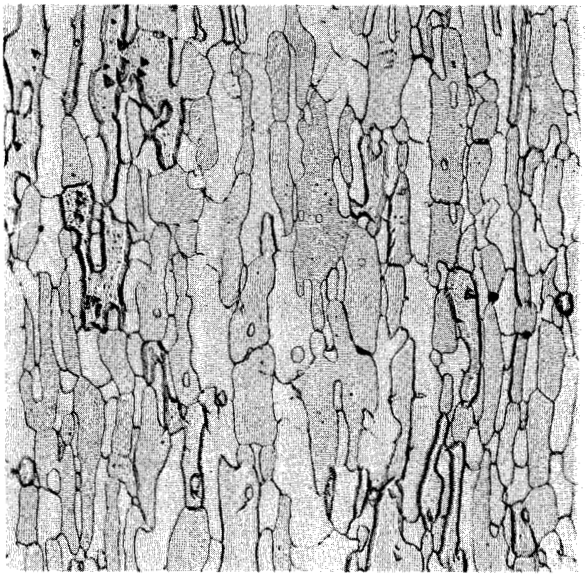

80% W Annealed 1400°C for 21 h.
Hardness HRC 27

90% W Annealed 1400°C for 21 h.
Hardness HRC 29

FIGURE 11. Typical Microstructures of 30%, 40%, 80%, and 90% W. Solid-state sintered and rolled to 0.1-in.-thick sheet. Longitudinal, 500X.

TABLE 4. Powder Sizes

Billet Numbers	Particle Size, μm			
	W	Ni	Fe	Cu
1C, 2C, 3F, 4F	30	45	45	61
1FP, 2FP, 80FP, 85FP, 90FP	4.78	7	4.37	

The second group of HERF billets was fabricated from the powders purchased specially for this program (Table 2). Billets made from these powders are identified as 1FP, 2FP, 80FP, 85FP, and 90FP, as shown in Table 4.

The powders were blended in a twin-shell blender for one hour with the intensifier bar running 1 min out of each 5 min. The powders were loaded into the HERF cans, shown in Figure 12, after which a load of 10 tons was applied. The surface of the packed powder was scratched and roughened and more powder was added to the cans. This process was repeated until the cans were full. The mild steel sleeve inside the can provided the effect of a heavy side wall and reduced wrinkling of the can side wall during consolidation. The loaded cans were dynamically evacuated for 0.5 h before preheat and during the 1.5-h preheat. A sufficiently long rubber evacuation tube allowed the billet to be transferred to the impaction die without disconnecting the vacuum pump. The stainless steel evacuation tube was sheared and flattened during the impaction stroke.

Impaction was performed using a 225,000 ft-lb Dynapak®. The billets that were impacted for this investigation are shown in Table 5. The copper-containing billets were impacted at 950°C, and the iron-containing billets at 1200°C. Two levels of energy were used on the first four billets. In each test the higher level, 123,750 ft-lb, showed a slightly higher density. Consequently, the five remaining impactions were made at 123,750 ft-lb. Density values of the impacted billets ranged from 97.7% to 99.3% of theoretical. Annealing of

® Registered trademark of General Dynamics, Inc.

TABLE 5. Billet Consolidation by HERF

Billet Number	Composition, wt% W	Ni	Fe	Cu	Impact Temperature, °C	Energy, ft-lb	Hardness, Rockwell "C" As-Hit	Annealed	Density, %
1C	36	45		19	950	112,500	B83	B48	98.2
2C	36	45		19	950	123,750		B70	98.6
3F	40	42	18		1200	112,500	C23	B85	97.7
4F	40	42	18		1200	123,750		B83	97.9
1FP	40	42	18		1200	123,750	C22		98.1
2FP	40	42	18		1200	123,750	C26	B92	99.3
80FP	80	14	6		1200	123,750		C26	
85FP	85	10.5	4.5		1200	123,750		C28	98.5
90FP	90	7	3		1200	123,750		C29	98.4

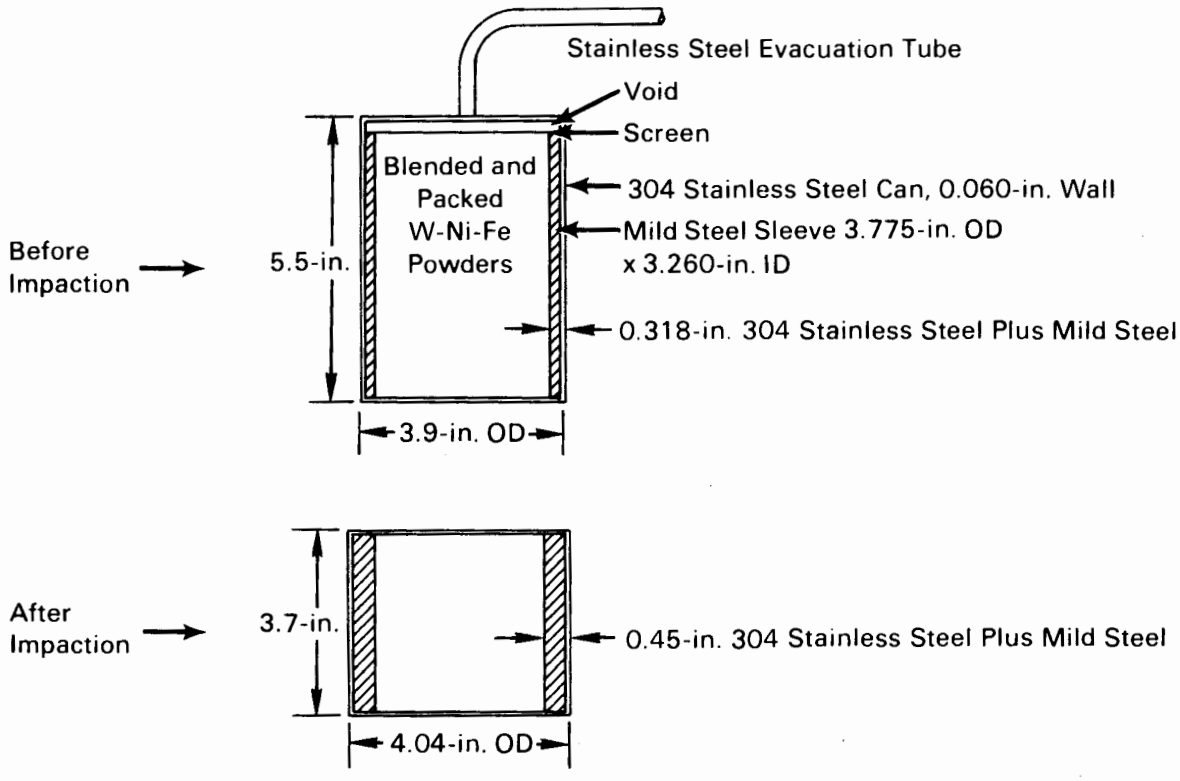

FIGURE 12. HERF Billet Assemblies

the impacted copper-containing billets at 1250°C or 1300°C, and of the iron-containing billets at 1400°C for 16 h in hydrogen, lowered the billet hardness considerably.

ROLLING HERF BILLETS

All rolling was performed on a two-high 14 x 14-in. mill and all reductions per pass were limited to 10% or less. The first four billets were cut into samples about 0.5 x 1.0 x 1.0 in. and used as trial pieces for rolling. Attempts to roll the W-45Ni-19Cu alloy in the as-impacted condition at room temperature resulted in only an 8% reduction at failure. Rolling this material at 500°C and 700°C resulted in a zero percent reduction at failure; annealing at 1300°C for 4 h in vacuum and then rolling at room temperature, 350°C, and 450°C also resulted in zero percent reduction at each temperature. It was therefore concluded that this alloy was not amenable to sheet rolling, and no further work was performed.

Attempts were also made to roll the W-42Ni-18Fe alloy in the as-impacted condition. Samples rolled at room temperature and 500°C showed zero percent reduction at each temperature. Best results were obtained when the W-42Ni-18Fe alloy was annealed at 1400°C for 3 to 6 h in hydrogen before rolling. Rolling tests were made on the annealed material at room temperature, 250°C, 500°C, and 900°C. No reductions without cracking were achieved in the 250°C and 900°C tests. Reductions at room temperature ranged from 5% to 8% on five specimens, and reductions at 500°C ranged from 11% to 53% on 17 specimens. It became clear that the best temperature for working this material was 500°C. The problem was the lack of consistency in the amount of warm work that the material would take before cracking. This made it difficult to design a processing schedule with an optimal number of anneals.

A second batch of powders was received in which the particle sizes were 6 to 10 times smaller (Tables 2 and 4). Billets 1FP and 2FP were consolidated from these powders using the same procedures previously described (Table 5). Rolling tests of portions of these billets showed that the annealed material could be rolled up to 70% reduction at 500°C before cracking. In one test, 71%

reduction was achieved by rolling at room temperature. It was also shown in these tests that reductions of 27% to 39% could be consistently achieved without cracking by rolling at 500°C.

Samples from billets 2FP and 1FP were rolled at 500°C to 6.3 x 9.0 x 0.100-in. thick in accordance with the schedule shown in Table 6. Material from these two sheets was used for mechanical testing.

Large differences are evident in the microstructure of billets produced from the old, coarse (OC) and the new, fine (NF) powders, as shown in Figure 13. Billet material made from the OC-particle powders shows considerable void volume and large grains in both the iron- and copper-containing alloys. The iron-containing alloy has a considerable amount of what appears to be a nonmetallic (probably oxide). Billet material made with the NF-particle powders has very fine tungsten particles distributed in a fine-grained, clean, void-free Ni-Fe matrix. These factors are undoubtedly responsible for the much improved rolling performance of the billets made from the NF powders.

Billets of 80%, 85%, and 90% tungsten (balance 70Ni-30Fe) were made from the NF powders and identified respectively as 80FP, 85FP, and 90FP. Samples of each of these compositions were rolled at room temperature, 500°C, 700°C, and 900°C.

TABLE 6. Rolling of HERF-Consolidated 40W-42Ni-18Fe Alloy Sheet at 500°C

Sample Number	Thickness at Start,[a] in.	Thickness at Finish, in.	Percent Reduction[b]
2FP	1.009	0.529	47.6
	0.529	0.308	41.8
	0.308	0.155	49.7
	0.155	0.100	35.5
1FP	1.263	0.743	41.2
	0.743	0.503	32.3
	0.503	0.298	40.8
	0.298	0.170	43.0
	0.170	0.098	42.4

(a) After annealing at 1400°C for 3 to 6 h in 50% H_2/50% Ar.
(b) Reductions per pass were 10% or less.

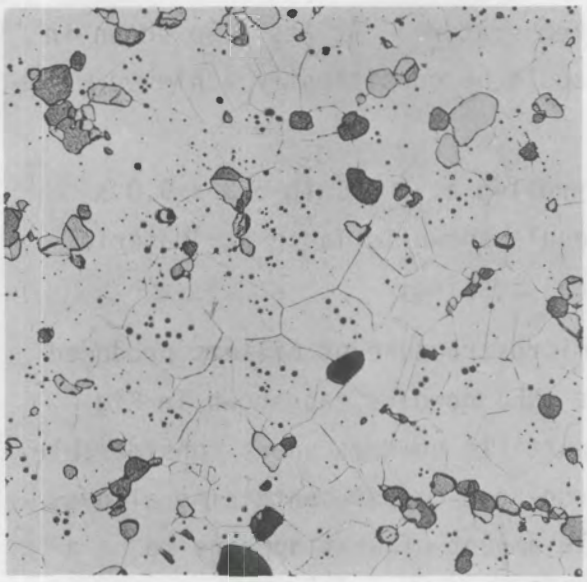

a) 40W-42Ni-18Fe Old Coarse Powder

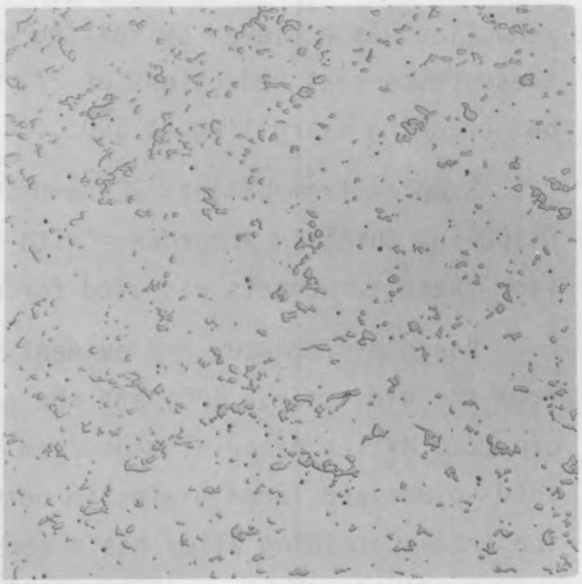

b) 40W-42Ni-18Fe New Fine Powder

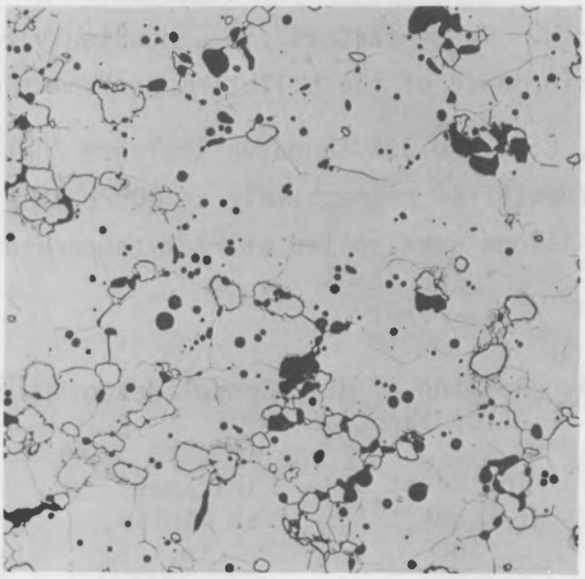

c) 36W-45Ni-19Cu Old Coarse Powder

FIGURE 13. Microstructural Differences Due to Powder Particle Size in HERF-Consolidated and Diffusion-Annealed Billets. Magnification 100X.

Best results were obtained with 80% tungsten at 500°C, at which reductions of 15% to 51% were achieved. A limited amount of reduction was achieved with the 80% tungsten alloy at room temperature and 700°C; at 900°C the 80% tungsten alloy could not be rolled without experiencing deep cracks in the edges and ends of the billet.

Best results with the 85% tungsten alloy were also obtained at 500°C, at which reductions of 6% to 46% were achieved. At room temperature and 900°C, the 85% tungsten alloy cracked; and at 700°C only 4% reduction was obtained before cracking. Microstructures of the 85% W alloys made with the NF tungsten powders are shown in Figure 14. The HERF-compacted and diffusion-annealed material has fine W particles distributed in a Ni-Fe-W matrix. The W particles became elongated during warm rolling 46% and retained their elongated appearance after annealing. Recrystallization is evident within the annealed tungsten particles.

The 90% tungsten alloy could not be rolled at any of the temperatures; therefore, no additional rolling attempts were made with this alloy.

Billets of the 80% and 85% tungsten alloys large enough (1.3 x 2.8 x 3.1 in.) to produce 0.1-in.-thick sheet for mechanical properties were machined from the same impacted and annealed cylinders. Attempts to roll these billets at 500°C failed after the first pass, which was about a 7% reduction. Presumably the narrow, thick billet was not compatible with the rolling process. No further work was attempted with these compositions.

Average hardness values obtained from the rolling are plotted as a function of percent of warm reduction in Figure 15. Maximal hardness is reached at about 30% reduction for the 80% and 85% W alloy.

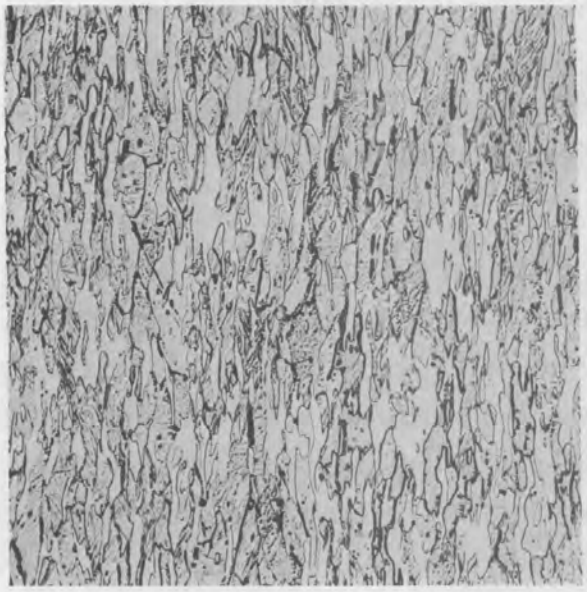

a) As-Rolled, 46% at 500°C

b) As-Annealed at 1400°C for 5 h, After Rolling 46%

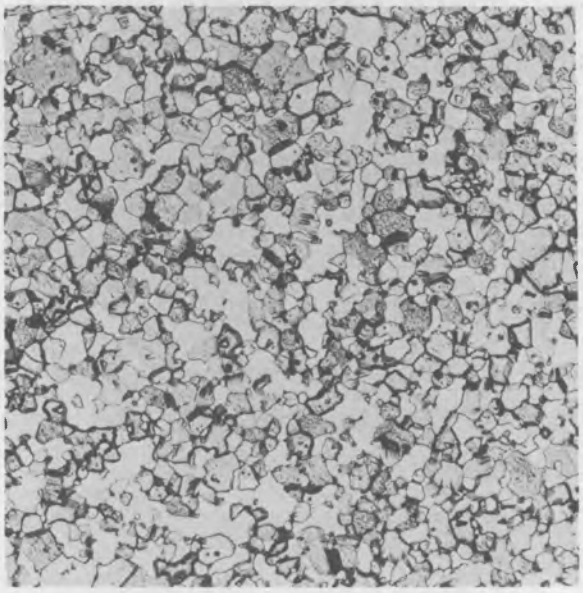

c) As HERF-Consolidated and Diffusion-Annealed

FIGURE 14. Typical Microstructures of 85W-10.5Ni-4.5Fe from HERF-Consolidated Billet. Made from NF powders. Magnification 250X.

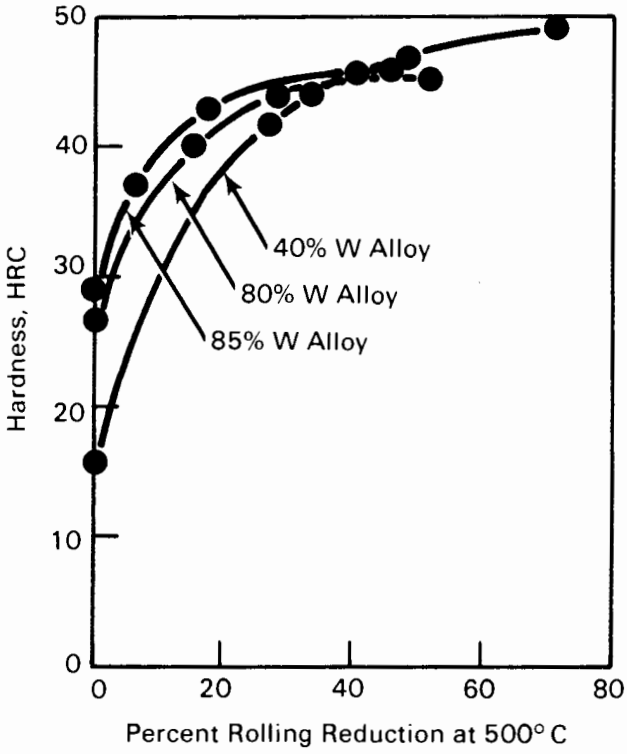

FIGURE 15. Hardness of HERF-Consolidated and Warm-Rolled W-Ni-Fe Alloys

ANNEALING

In their original work with W-Ni-Fe heavy metal alloys, Green, Pitkin, and Jones (1954) found that alloys containing 75% to 90% W readily rolled with reductions of 60% in cross sectional area between anneals. For intermediate anneals, it was found necessary to heat treat the material at 1440 to 1460°C to ensure subsequent reductions of 60% without crack development. Their work was on small (1.5 x 6 x 0.125 in. thick) LP-sintered billets. Because SS-sintered billets have a distinctly different microstructure, they are generally more brittle than LP-sintered billets (O'Neil and Salyer 1964). Therefore, intermediate annealing heat treatment is particularly important to the rolling of SS-sintered billets.

Frantsevich et al. (1967) annealed LP-sintered 90% W (with 2% to 59% cold work) for 1 h. They found that the recovery, recrystallization, and attendant hardness loss were definitely related to the prior amount of cold work. Generally, the loss in microhardness occurred over a temperature range of 600 to 1300°C for the W phase and 200 to 1000°C for the matrix.

To determine the optimal annealing cycles for this work, a series of experiments were run on commercially available rolled 0.033-inch-thick 91% W sheet[(a)] that had a final anneal at 1100°C for 20 h. All annealing was done in cold wall furnaces with a 50% H_2/50% Ar atmosphere. Changes in hardness and impact energy were measured as a function of annealing temperature and time. The measured impact energy is the energy absorbed by the material in a three-point bending test under dynamic loading conditions. The test is actually a modified Charpy impact test using an unnotched specimen with the load applied normal to the rolled sheet face. An instrumented impact system was utilized which provided a complete temporal load and energy history of the impact event. The impact energy is largely a function of dynamic ductility, since the loads recorded during the test do not vary much, while the total specimen deflection increases significantly as impact energy is recovered by annealing. The results are summarized in Figure 16.

(a) From Teledyne Firth Sterling, Nashville, Tennessee.

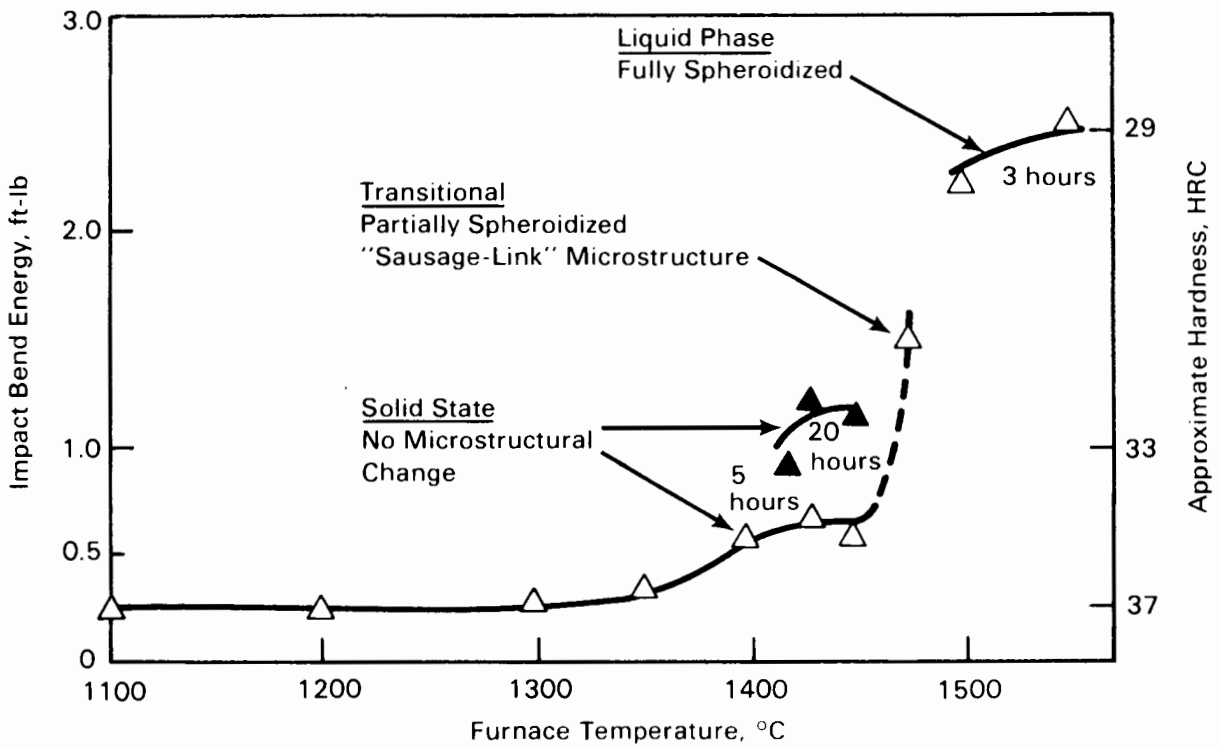

FIGURE 16. Impact-Bend Energy as a Function of Annealing Temperature and Time

No significant improvement in properties occurred below 1400°C. In the 1400 to 1450°C range there is a decided improvement in impact energy, especially as time is increased from 5 to 20 h, but there is no observable change in microstructure compared to the as-received condition, 1100°C for 20 h (see Figure 17). At 1475°C furnace temperature (about 1450°C sheet temperature), there is a definite jump in impact energy, and the tungsten phase has begun to coalesce as evidenced by the "sausage link" structure shown in Figure 17. This transitional structure probably indicates the onset of melting. Such structures are undoubtedly difficult to reproduce, especially in large-area sheets, because of the need to maintain temperature within an absolute range of a few °C. At 1500 to 1550°C for 3 h the impact energy has made another jump and the structure is fully spheroidized. In this temperature range the matrix is fully molten, making shape retention difficult, and in alloys of less than 80% W the tungsten phase will segregate.

It was decided, therefore, that the best practical annealing temperature is a furnace temperature of 1400°C. By varying the time at temperature

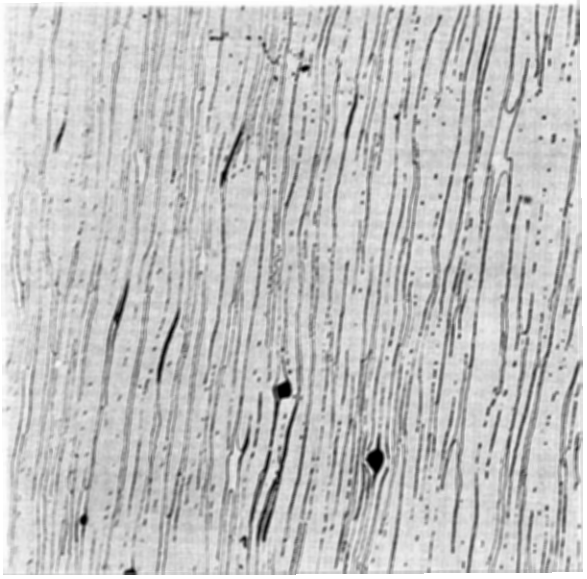

a) 1100°C for 20 h
Hardness HRC 37

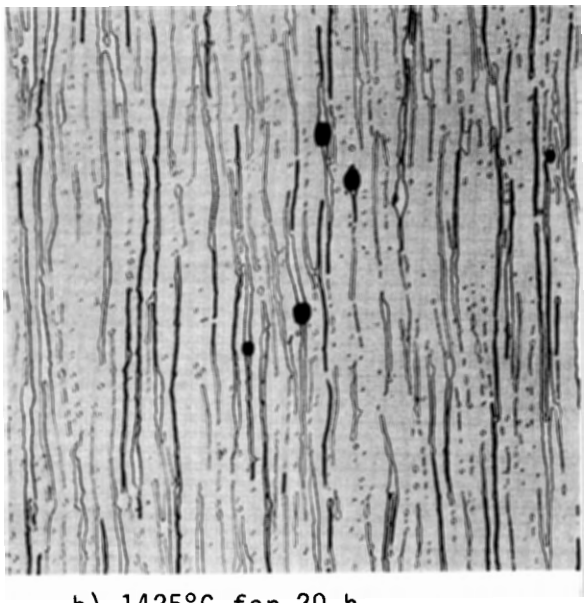

b) 1425°C for 20 h
Hardness HRC 32

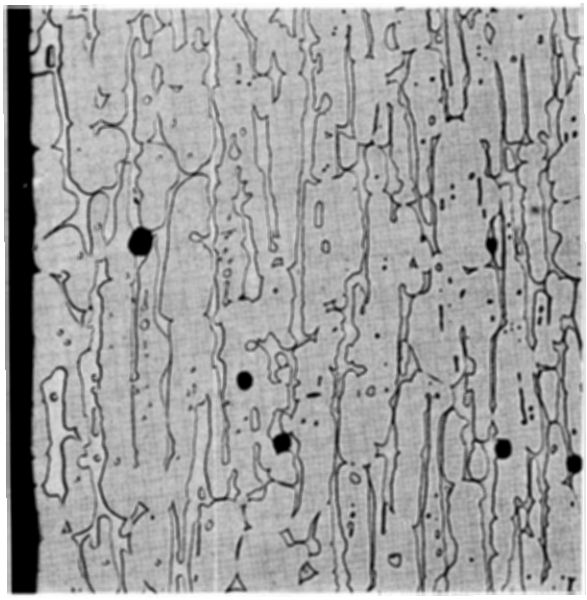

c) 1475°C for 5 h Partially
Spheroidized Hardness HRC 30

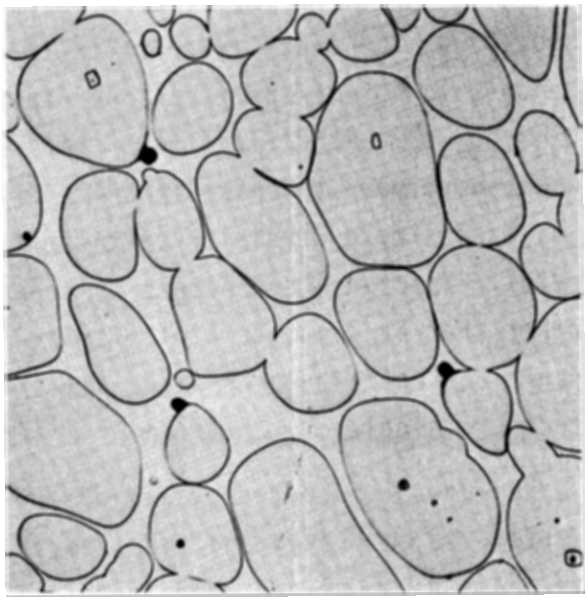

d) 1500°C for 3 h Spheroidized
Hardness HRC 29

FIGURE 17. Microstructure of Rolled 91% W as a Function of Annealing Temperature and Time. Polished, longitudinal sections 250X.

depending on the total tungsten content, a substantial recovery of ductility is made while avoiding any melting due to nonuniform temperature distribution in the furnace. Most intermediate anneals were held for 3 to 5 h at 1400°C in 50% H_2/50% Ar. Frequently, the time was cut to 1 or 2 h for the 30% and 40% W alloys because they have such a small amount of tungsten phase.

German, Hanafee, and DiGiallonardo (1984) have shown that rapid quenching from annealing temperatures gives superior toughness, probably due to decreased impurity segregation at the W-matrix interface. All material in this study was furnace cooled from 1400°C to ~500°C in around 5 min, which roughly corresponds to the moderate cooling rate employed by German et al. Their moderate cooling rate yielded unnotched Charpy impact energies 2 or 3 times those of as-sintered material, which are in agreement with our results (shown in Figure 16). In comparison, their rapid cooling rate (to 200°C in less than 20 seconds) yielded impact energies 5 to 15 times those of as-sintered material.

All anneals by German et al. were for 2 h in vacuum. Figure 16 indicates a further improvement in impact energy upon increasing the annealing time from 5 to 20 h. The exact reasons for the improvement are unknown; however, a brief transmission electron microscope examination of material annealed for 5 and 20 h showed fewer dislocations remaining in the W grains after the longer annealing time. Yodogawa (1982) showed that, in alloys annealed at 1420°C for 1 h, each single crystal W particle fully recrystallizes into several new grains. Fracture then occurs by separation of these recrystallized grains rather than by cleavage of the entire particle. Perhaps grain growth that occurs during longer annealing times tends to return the W particle to the stronger, single-crystal form.

An unexplained defect was observed in the 70% to 90% W sheets after all rolling was completed and the sheets were annealed at 1400°C for 16 to 20 h. The surface became depleted in matrix and the remaining tungsten grains underwent considerable growth, as shown in Figure 18. Since this defect did not appear in the as-sintered sheets, it must have occurred during annealing, and it was probably enhanced by repeated rolling and annealing as well as the very long final annealing time. The defect was not observed in 30% and 40% W sheets; their final anneals were only 1 to 4 h. Besides time and temperature

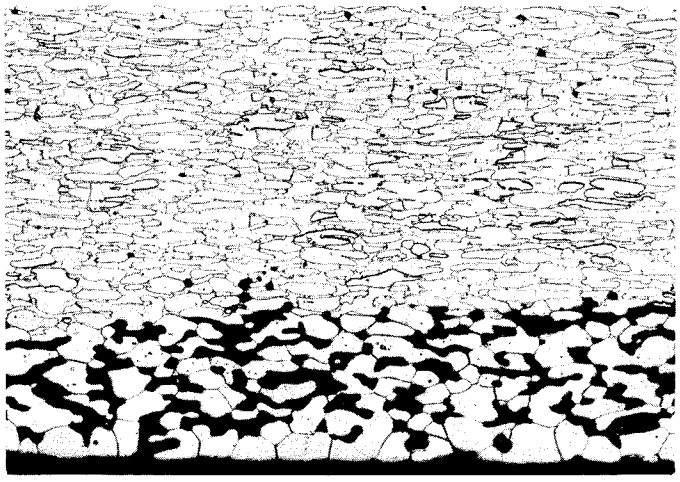

a) Unusual, two-of-a-kind defect. Matrix has disappeared, leaving a W skeleton. This sheet was rolled from a LP-sintered, 85% W billet. Another 90% W sheet had a similar surface 4 mil deep.

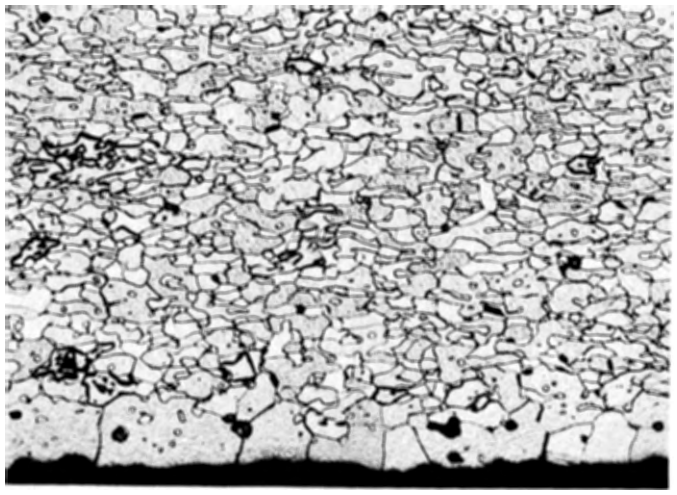

b) Typical surface on all 70% to 90% W sheets after rolling and annealing at 1400°C for 16 to 21 h. Typically ~1 mil thick; one sheet rolled from a 90% W SS-sintered billet had a layer 5 mil deep. Probably an annealing defect. Not observed in 30% and 40% W sheets. Not present in as-sintered billets.

FIGURE 18. Matrix Depletion and W Grain Growth at Rolled and Annealed Sheet Surfaces

of annealing, surface contamination could contribute to formation of this defect. Contamination could come from the rolling mill or from the refractories used during annealing. In most cases the depth of the defect was only about 1 mil, but there were single sheets having defect depths of 5 and 7 mil. The extent to which these defects affect mechanical properties is not known, but their presence should be considered in interpreting the mechanical property data given in the following section.

STRAIN AGING AND PRECIPITATION HARDENING

Tungsten-nickel-iron alloys exhibit two distinct aging phenomena, precipitation hardening of the matrix and strain aging.

In 90% W alloys strain aging occurs in the 400 to 600°C range. Hardness increases approximately 3 to 5 points Rockwell C (HRC) on aging material that has been previously cold worked 25% (Penrice 1980). Correspondingly, tensile ultimate strength increases from 170 to 210 ksi and elongation decreases from 8.5% to 2.5% (Myhre 1980). Wehr (1962) was probably the first to identify this aging phenomenon. Although no precipitates have been identified in tungsten heavy metal alloys that have been strain aged (Penrice 1980), the occurrence of strain aging in W has been well documented (Wehr 1962; Stephens et al. 1964). Due to the high vol% W phase in the 90% W alloys, the strain aging responsible for the significant property changes must occur largely within the W phase.

Frantsevich et al. (1967a, b) upset cylinders of 90% W in a semi-isostatic medium and annealed them at 400 to 1350°C and found no indication of age-hardening in either the matrix or the W phase. Based on microhardness measurements of cold rolled and annealed 90% W, Yodogawa (1982) observed maximal hardness in the W phase at 700°C and attributed it to strain aging. The maximal matrix hardness, attained at 500°C, was attributed to segregation of W in the matrix phase, although no microscopically observable precipitate was noted.

The equilibrium solubility of W in the Ni-Fe matrix varies from a maximum at the solidus (~1460°C) of about 30 wt% W (Wehr 1962) to 15% to 20% W in the temperature range of 1150 to 800°C (Agababova and Chaporova 1969; Henig, Hofmann, and Petzow 1981). Typically, 90% W alloys are heat treated near 1100°C to improve ductility (Myhre 1979; Muddle and Edmonds 1983; Lux, Jangg, and Danninger 1981); the resulting matrix W composition is 21% to 23% (Northcutt 1975; Bukatov, Romashov, and Gostev 1983). Because of this variation in W solubility with temperature, hardening of the matrix by W precipitation becomes a definite possibility. However, these W precipitates have not been found in normally processed 90% W heavy metals; only in specimens quenched from a sintering temperature of 1550°C (Bukatov, Romashov, and Gostev

1983). Presumably, the diffusion distances through the matrix in 90% W alloys are so short that the excess W deposits out on the surface of the existing W spheroids. This W deposition probably occurs during cooling from sintering, leaving little or none of the excess W required for precipitation-hardening. The matrix in low-W alloys does retain sufficient W content for precipitation hardening to take place, as described below.

A series of aging experiments were conducted using the 40% W alloy, the matrix of which should be metallurgically similar to that present in all higher-W alloys; that is, the excess W content (about 10%) ensures complete saturation of the matrix with W, and the coarse W dispersion (remaining ghosts of the original W powder particles) prevents excessive matrix grain growth. Also, any large property changes would be attributable to the matrix.

Initially, a single piece of SS-sintered 40% W alloy (fast furnace cooled) was cold worked 71% by rolling. This piece was then aged for a half hour at 300°C, and then at 100°C increments up to 1400°C. The resulting aging behavior was monitored by changes in hardness (HRC), as shown in Figure 19. The upper curve for the 71% cold worked material displays a hardness increase of 3 points HRC due to strain aging in the temperature range from 400 to 600°C. Above 600°C, hardness drops off rapidly as the matrix anneals, but between 1000°C and 1100°C hardness again increases 2 points HRC as W precipitates harden the matrix. Above 1200°C, hardness drops rapidly as overaging allows full annealing to occur. This same piece of material was fully annealed at 1400°C for 4 h (fast furnace cooled) and then given the same series of aging treatments, shown in the lower curve of Figure 19.

In the fully annealed 40% W there is no change in hardness up to 900°C, where precipitation-hardening again takes place. A gain of some 16 points HRC brings the peak hardness at 1000°C to essentially the identical hardness peak experienced in the 71% cold worked condition. There was no hardness increase in the 400 to 600°C range, indicating that the hardening previously experienced in the 71% cold worked condition is due to strain aging. To further test this hypothesis, the same piece of material was reannealed at 1400°C for 4 h, cold

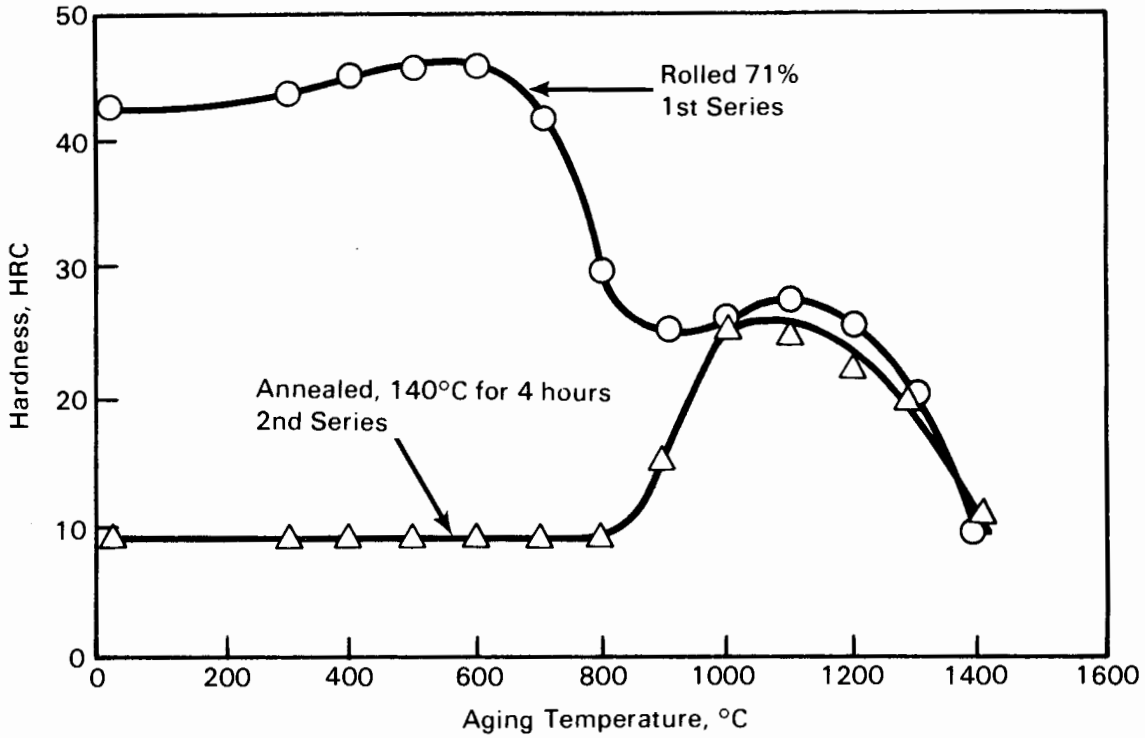

FIGURE 19. Age Hardening Behavior of 40% W. One sample, aged for 1/2-h at each temperature indicated, beginning at room temperature and progressing upward.

worked 45% by rolling, and subjected to the same series of aging treatments for a third time. The as-rolled hardness of HRC 39 increased 2 points maximum in the 400 to 600°C range, somewhat less, as expected, than the 3-point increase experienced in the more severely worked 71% cold worked condition.

Up to 900°C heating could be performed in air, since only thin oxide films formed in a half hour. Above 900°C, aging was performed in a vacuum to avoid thick, loose oxide films.

The strain aging response of 40% W in the 71% cold worked condition is shown in Figure 20. Maximal hardness (~45 HRC) is reached in 4 to 20 h at 450°C, in 1 h at 500°C, and in only a quarter hour at 600°C. At 600°C over-aging occurs rather rapidly. These data indicate that the matrix strain ages to maximal hardness under time and temperature conditions similar to those used by Myhre (1980) for 90% W. It follows then that both the matrix and the W phase can strain age. However, the strain aging response of the matrix was found to vary in later tests, as shown in Figure 21. Here material from

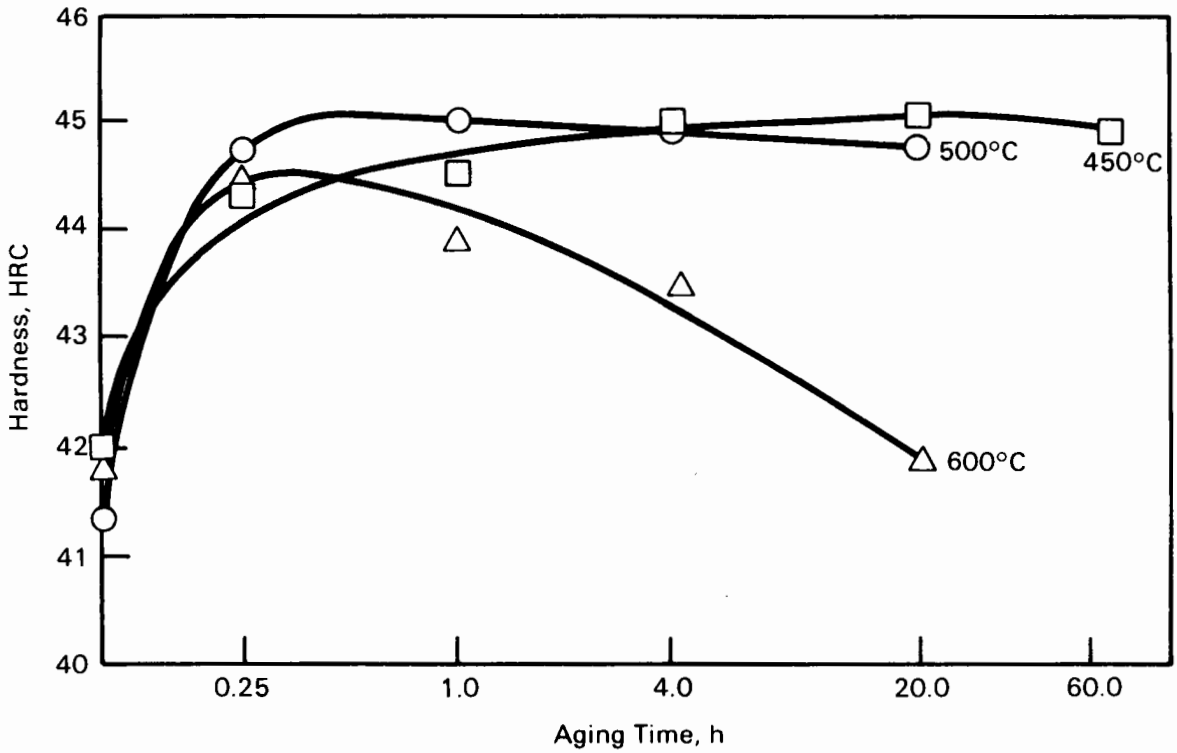

FIGURE 20. Strain Aging Response of 40% W after 71% Rolling Reduction as a Function of Time and Temperature

several 30% and 40% W sheets was aged at 482°C and the hardness was monitored over time. Only the 69% and 71% cold worked 40% W hardened, about 2 to 3 points. Neither the 46% cold worked 30% W nor the 32% cold worked 40% W appeared to harden at all. This variable strain aging response remains unexplained. Perhaps high concentrations of O, N, C, or some other impurity are required, along with a high degree of cold work. Or perhaps strain aging does not occur at all in pure powders that are sufficiently deoxidized and decarburized during the sintering cycle. In any event, the amount of hardening obtained by strain aging the low-W compositions is minimal. Therefore, no mechanical properties tests were run on strain aged material in this study. Instead, efforts were directed toward precipitation hardening, which appears to have a more significant influence on mechanical properties.

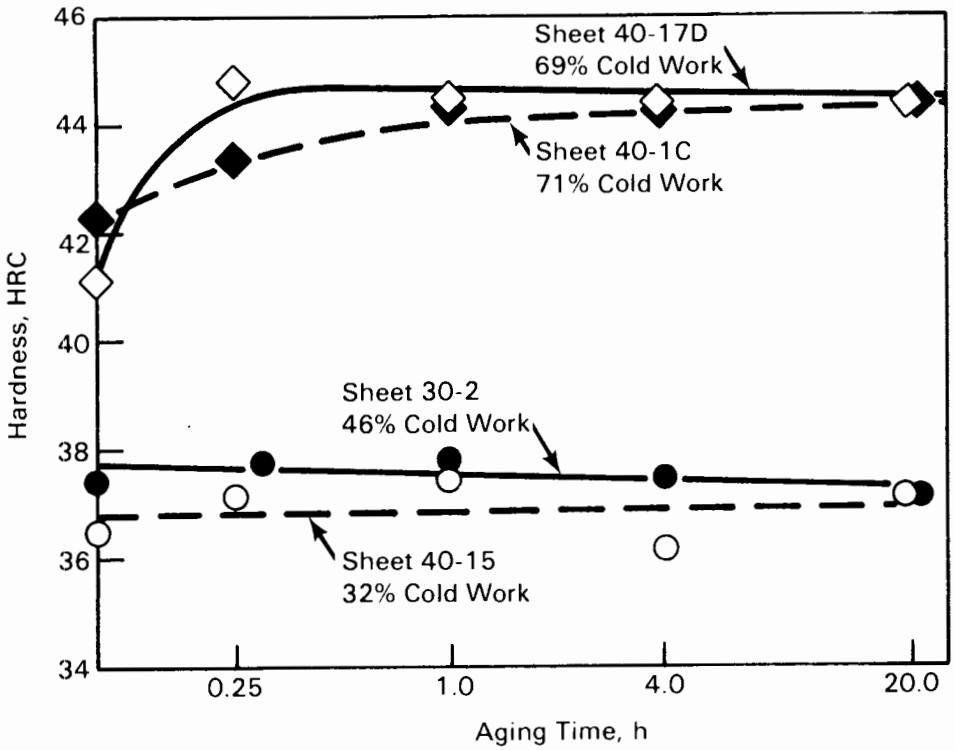

FIGURE 21. Strain Aging Response of 30% and 40% W Sheets at 480°C as a Function of Time

The precipitation hardening response of 40% W is shown in Figure 22. Maximal hardness (~24 HRC) is reached in a half hour at 1050°C, 3 h at 925°C, 10 h at 850°C, 20 h at 800°C, or 40 h at 750°C. Overaging begins after 1 h at 1050°C, and at 20 h the lamellar W precipitates have started to spheroidize, as shown in Figure 23. At 1050°C about 60% of the microstructure contains coarse lamellar precipitates; grain boundary precipitation of W is evident elsewhere. The precipitation at 925°C is nearly uniform throughout the microstructure and the lamellae are finer. The mechanical properties of this material, aged for 2 h at 1050°C and 925°C, are reported in the next section, along with the properties of annealed and cold worked material. No mechanical properties were measured on samples aged at 800°C and 750°C, but their microstructures (Figure 23d and e) are of interest. The material aged at 800°C has the most uniform precipitation of any of the samples, and the sample aged at 750°C has

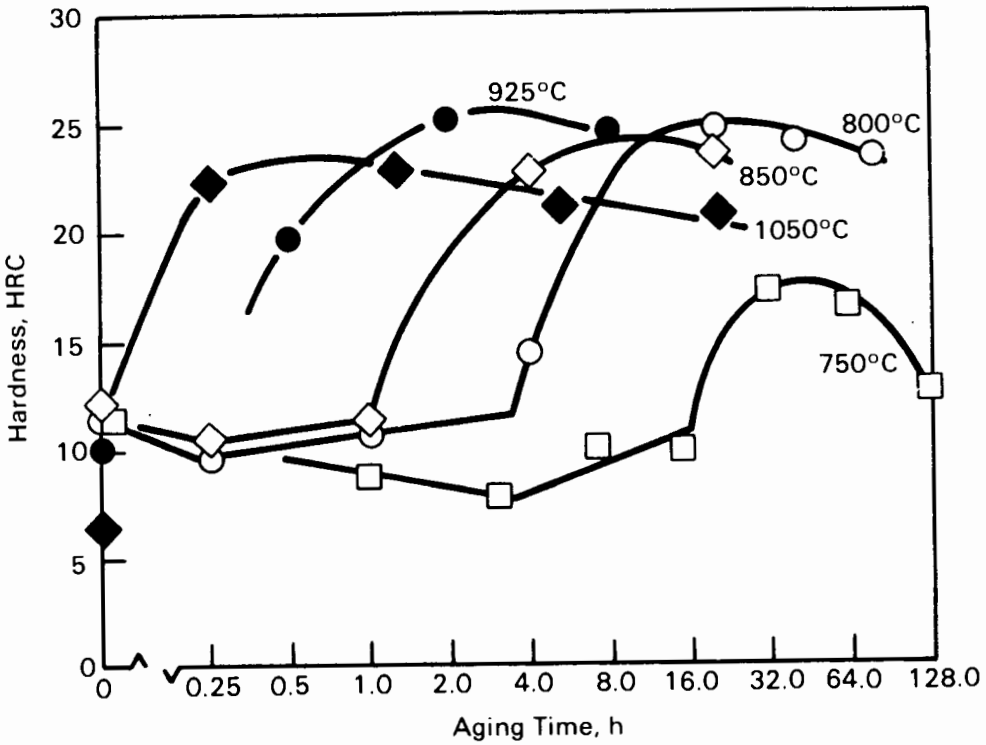

FIGURE 22. Precipitation Hardening Response of 40% W after Solution Annealing 4 h at 1400°C with Fast Furnace Cool

spotty precipitation similar to that of the sample aged at 1050°C. Apparently, the optimal precipitation hardening temperature is between 800°C and 900°C.

Attempts were made to identify the lamellar precipitate. The precipitate was too fine to be identified by EDAX on the scanning electron microscope. Samples of 40% W were also examined by x-ray diffraction both in the solution annealed condition and after precipitation hardening at 925°C for 2 h (microstructures shown in Figure 23). The diffraction patterns from both samples indicated only two phases, bcc W and fcc gamma solid solution (Ni-Fe-W matrix). No indication of a new phase was found. The amount of precipitate probably ranges from 3 to 8 vol% (based on W contents in the solid solution matrix of 25 to 30 wt% as solution annealed and 15 to 20 wt% after 2 h at 925°C), which is near the limits of detection by conventional x-ray diffraction. Others (Bukatov, Romashov, and Gostev 1983; Henig, Hofmann, and Petzow 1981) have identified similar precipitates, occurring under similar conditions, as W. Since we have been unable to contradict, or confirm, their findings, we have assumed that the precipitates found here are indeed W.

As indicated in Figure 22, there is a slight hardness drop during the incubation period which precedes the precipitation hardening reaction. The reason for this is not known.

The annealing-aging response of 40% W in the 31% cold worked condition is illustrated in Figure 24. At 800°C, 850°C, and 950°C the material softens rapidly at first and then assumes a hardness of about HRC 25 due to precipitation hardening. At 750°C the initial hardness drop is slower but the effects of precipitation hardening are diminished, and after 30 h the hardness is below that attained at higher temperatures. At 125 h the hardness is HRC 20. Apparently, very long times at 750°C would be required for the hardness to drop to that of fully annealed material, HRC 12.

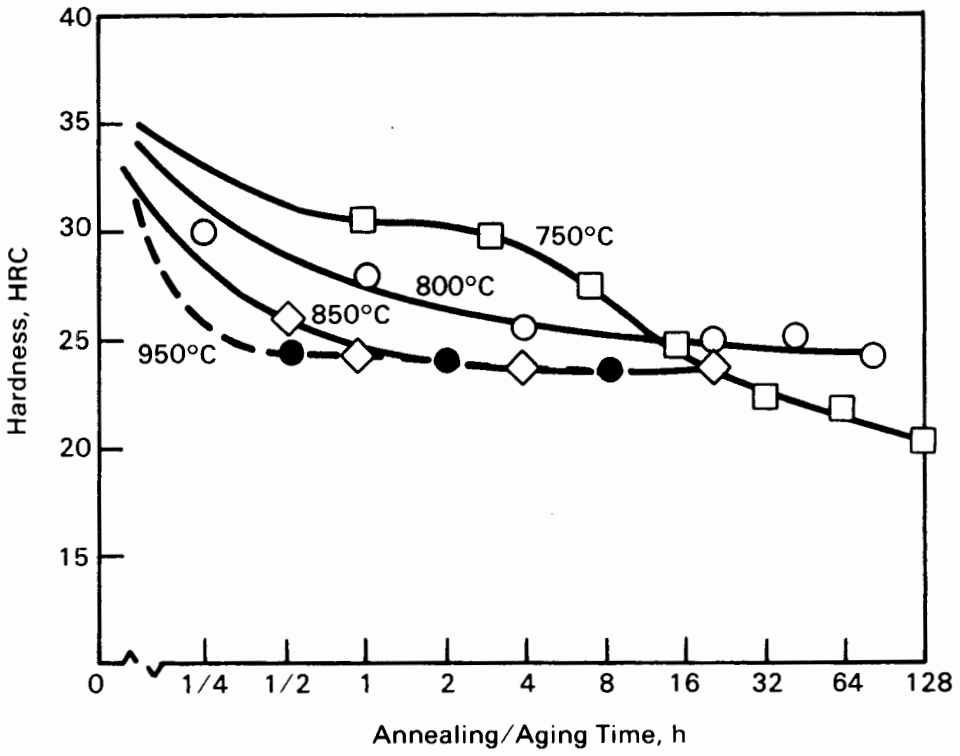

FIGURE 24. Annealing-Aging Response of Cold Worked 40% W, Rolled 31% after Annealing at 1400°C for 4 h

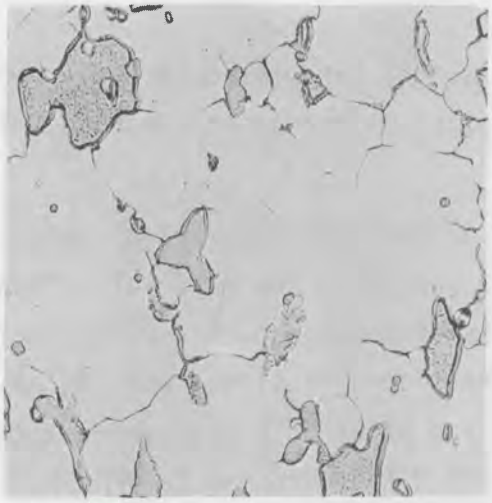

a) Solution Annealed, HRC 12

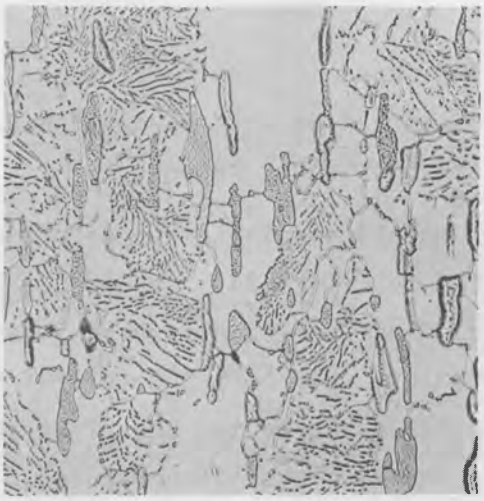

b) Aged 1050°C for 20 h, HRC 21

c) Aged 925°C for 2 h, HRC 26

d) Aged 800°C for 20 h, HRC 25

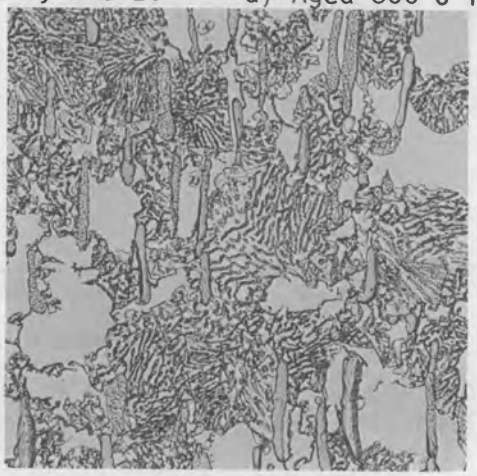

e) Aged 750°C for 32 h, HRC 17

FIGURE 23. Microstructures of Solution Annealed and Precipitation Hardened 40% W Sheet. Longitudinal, 500X.

MECHANICAL PROPERTIES

TEST METHODS

The mechanical properties of the heavy metal alloys were evaluated using standard tensile and Charpy V-Notch (CVN) tests. The tensile tests were performed in accordance with ASTM E8 using the 0.25-in. wide subsize sheet specimen. The machined edges of the 1.25-in.-long reduced section were sanded in the longitudinal direction with 600-grit SiC paper to provide consistent elongation results. The high notch sensitivity of the heavy metal alloy, plus the surface hardening that results from the machining operation, can cause premature failure of the specimens if the machined edges are not polished. The flat surfaces of the specimens had the as-rolled finish. The specimens were tested at 10^{-2} in./in. per minute to the yield point and then at 10^{-1} in./in. per minute to failure. Extensometry was used to determine the yield strength at the 0.2% offset and to estimate the modulus of elasticity.

Subsized CVN impact tests were performed in accordance with ASTM standard E23, with the exception that the impact velocity was less than prescribed. The width of the subsized specimen was limited to the sheet thickness, 0.1 in., while the remaining dimensions were unchanged. The specimens were tested on an instrumented drop tower impact machine at either 28 or 40 in. per second. The instrumented impact system was utilized because of the low energies absorbed by the specimens. In addition, the microprocessor-controlled instrumented impact system provided a complete temporal load and energy history of the impact event. The total energy absorbed by the specimen was normalized to a specimen width of 1.0 in. to compensate for variations in sheet thickness, and the results are reported here as ft-lb of energy absorbed per inch of specimen thickness.

RESULTS AND DISCUSSION

The measured mechanical properties of the sheet fabricated in this program are given in Table 7. Each data point is the average of three tests made for each condition and each orientation with respect to the final rolling

TABLE 7. Mechanical Properties Data

Sheet Number, Composition, Condition	Hardness, HRC	Orientation	Slow Tensile Ult., ksi	Slow Tensile Yield, ksi	Slow Tensile Elong., %	Slow Tensile Elastic Modulus, 10^6 psi	Impact CVN, ft-lb/in.
40-12B							
40% W, SS sinter	12	Long.	117	51.4	54.9	23.5	-
Annealed							
1400°C for 1 h		Trans.	120	51.1	58.2	27.5	94.4
40-17							
40% W, SS sinter	38	Long.	164	154.5	9.1	29.9	-
Cold rolled 29%							
		Trans.	164	143.5	8.3	29.8	40.1
40-17D							
40% W, SS sinter	21	Long.	132	60.9	42.2	28.2	114.9
Precipitation hardened							
1050°C for 2 h		Trans.	133	63.5	40.7	26.1	90.6
40-13 PH							
40% W, SS sinter	26	Long.	147	79.0	32.9	29.9	87.7
Precipitation hardened							
925°C for 2 h		Trans.	144	81.2	31.7	29.4	71.3
1-FP-40B							
40% W, HERF	13	Long.	123	54.3	55.1	28.5	124.8
Annealed							
1400°C for 3-1/2 h		Trans.	119	53.0	48.6	31.0	84.7
1-FP-40A							
40% W, HERF	40	Long.	171	163.3	6.5	28.3	49.0
Warm rolled 40%		Trans.	178	161.4	6.3	28.4	29.0
70-4							
70% W, SS sinter	24	Long.	122	75.4	18.0	28.3	-
Annealed							
1400°C for 16 h		Trans.	128	72.3	34.7	36.4	47.2
80-1							
80% W, SS sinter	25	Long.	117	78.4	14.0	36.5	-
Annealed							
1400°C for 16 h		Trans.	116	84.6	7.8	38.0	12.7

TABLE 7. (contd)

Sheet Number, Composition, Condition	Hardness, HRC	Orientation	Slow Tensile Ult., ksi	Slow Tensile Yield, ksi	Slow Tensile Elong., %	Slow Tensile Elastic Modulus, 10^6 psi	Impact CVN, ft-lb/in.
80-3							
80% W, SS sinter	28	Long.	130	81.4	20.2	44.1	14.4
Annealed							
1400°C for 21 h		Trans.	126	81.5	13.2	47.4	15.2
85-4							
85% W, SS sinter	29	Long.	124	81.5	20.0	38.9	5.1
Annealed							
1400°C for 16 h		Trans.	123	80.9	15.2	35.7	5.9
85-2							
85% W, LP sinter	26	Long.	116	75.7	19.7	37.5	11.8
Annealed							
1400°C for 21 h		Trans.	118	72.3	23.1	38.8	15.3
90-12							
90% W, SS sinter	29	Long.	111	79.1	8.6	34.6	2.3
Annealed							
1400°C for 21 h		Trans.	112	80.1	8.5	30.4	2.4
90-10							
90% W, LP sinter	28	Long.	113	79.5	14.0	40.8	10.9
Annealed							
1400°C for 21 h		Trans.	113	80.7	13.3	40.4	6.0

direction. Most of the data are for annealed sheet derived from SS-sintered and HERF billets. Comparative data are also given for 40% W in precipitation hardened and cold worked conditions and for 85% and 90% W sheet derived from LP-sintered billets. Important relationships among W content, sintering method, heat treatment, and mechanical properties are shown in Figures 25 through 29.

The relationships between W content and tensile properties for annealed sheet are shown in Figure 25. Ultimate strength is nearly the same for all W contents between 40% and 90%. Yield strength decreases slowly with W content, about 7 ksi for each 10% decrease in W content. Elongation increases rapidly toward lower W content, as expected. For SS-sintered material, elongation

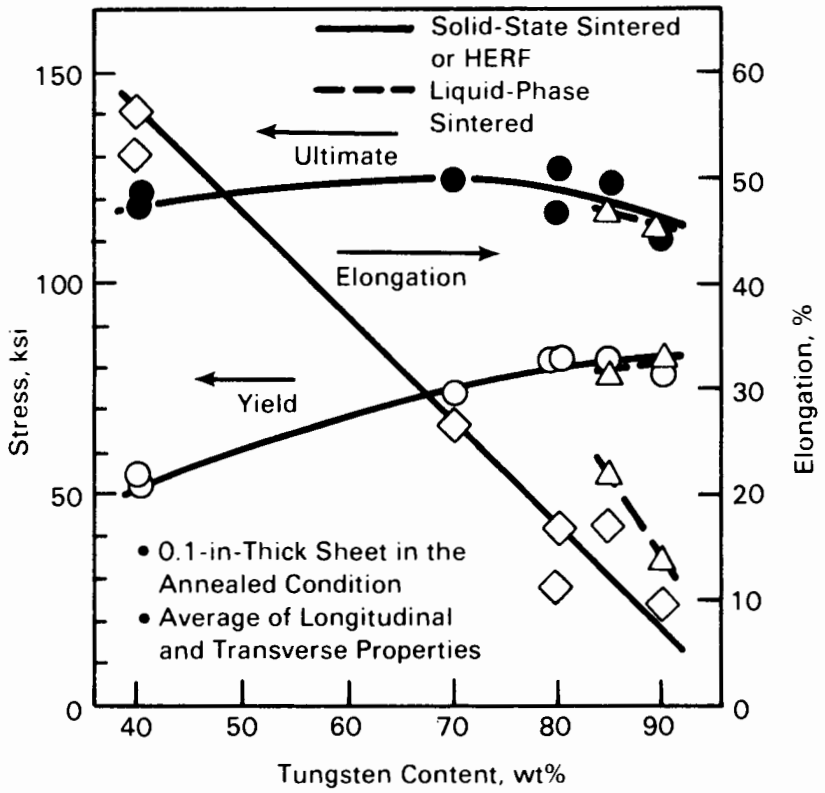

FIGURE 25. Tensile Properties of 40% to 90% Tungsten Alloys

increases about 10% for each 10% decrease in W content. Ultimate and yield strength values for LP- and SS-sintered materials are essentially the same, whereas elongation values for the LP-sintered materials (85% and 90% W) are roughly double those for the SS-sintered materials having the same W content.

Previous investigators from Takeuchi (1967) to Lux et al. (1982) have noted that SS-sintered 90% W is extremely brittle due to the interconnected W skeleton (high contiguity). For a typical comparison of LP- and SS-sintered microstructures see Figure 9. Churn and German (1984) state that the maximum attainable elongation in LP-sintered material depends on contiguity (frequency of W-W contact in the microstructure), which in turn is set by the alloy composition (W content). For the SS-sintered material of the same W content, the contiguity is obviously higher and the ductility is logically, and in fact, lower. As the 0.5-in.-thick billets were rolled to 0.1-in.-thick sheet, the microstructures of the LP- and SS-sintered material became more alike, as shown

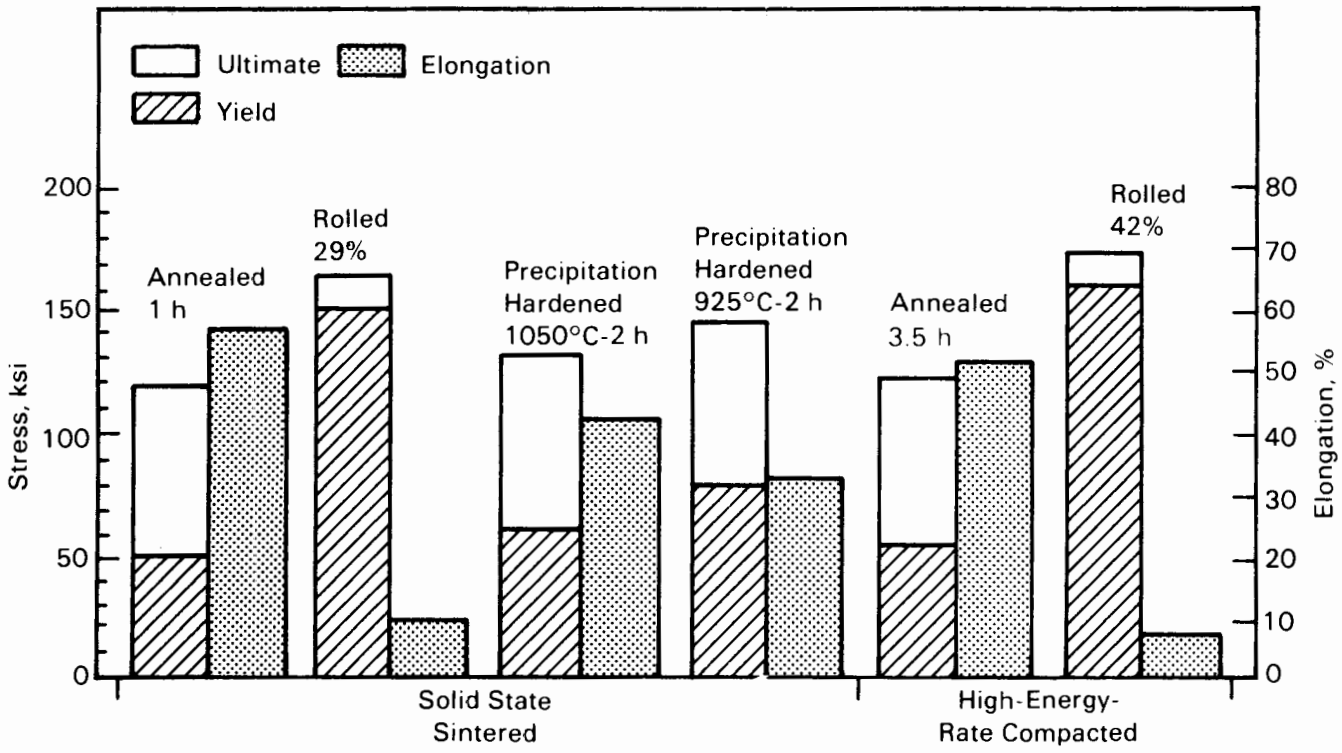

FIGURE 26. Tensile Properties of 40% Tungsten Alloy. Longitudinal and transverse values averaged.

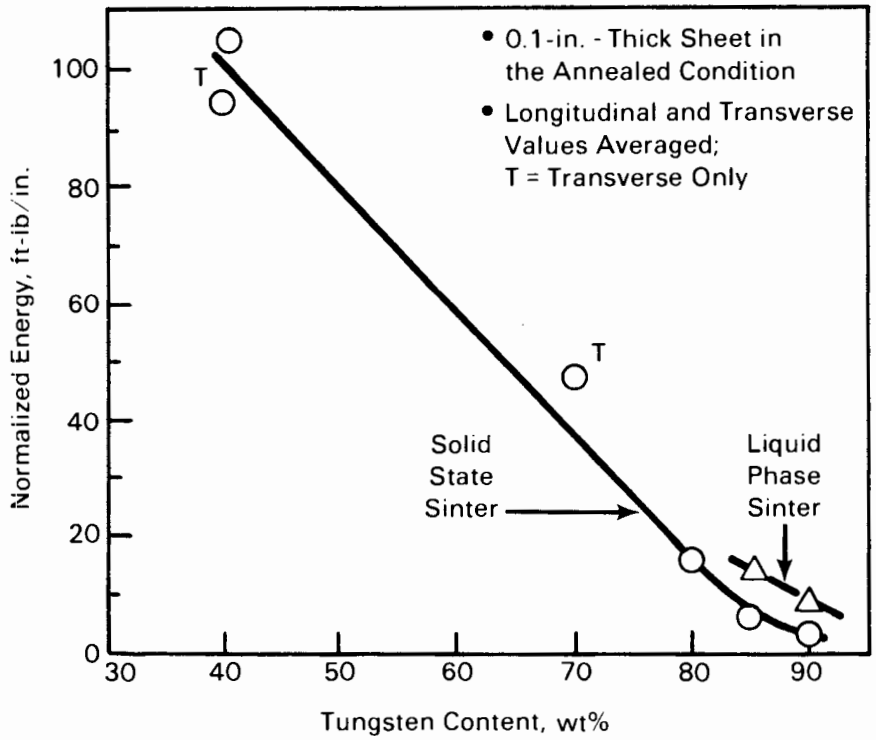

FIGURE 27. CVN Impact Energy as a Function of Tungsten Content

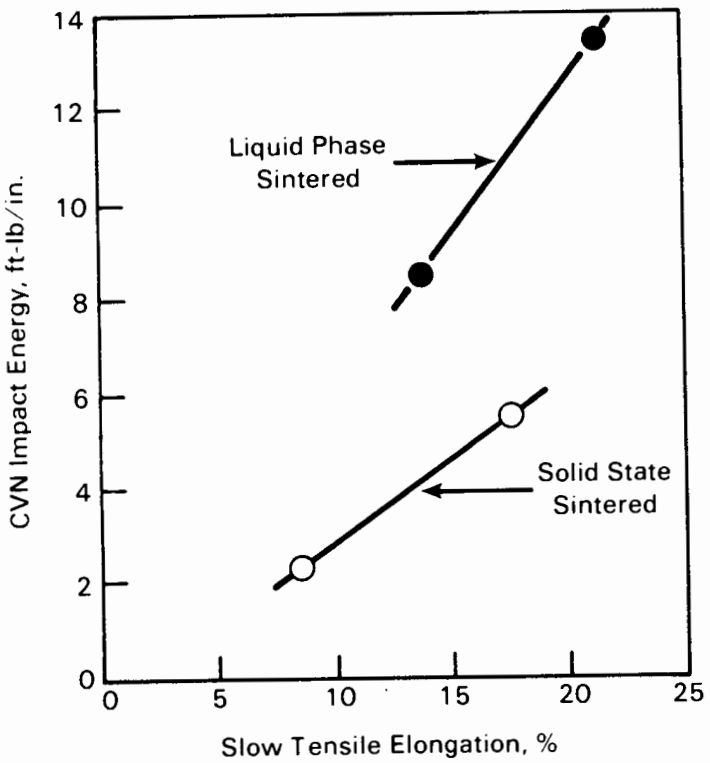

FIGURE 28. CVN Impact Energy as a Function of Tensile Elongation for LP- and SS-Sintered 85% and 90% W Alloys

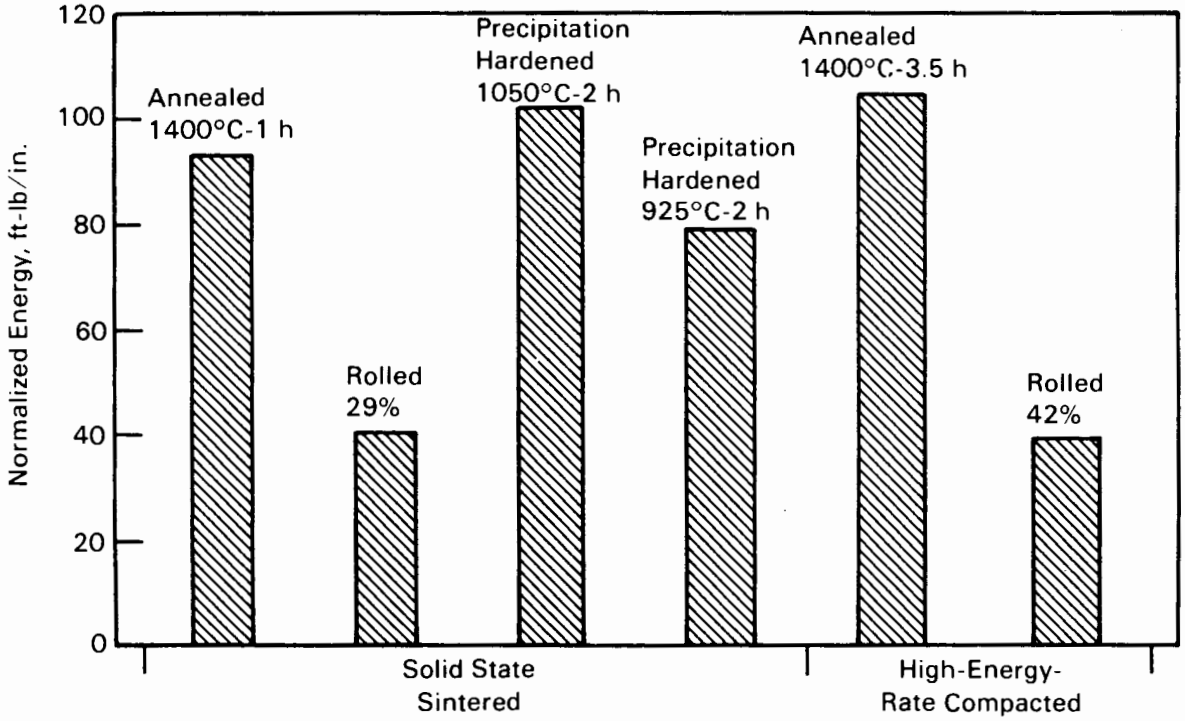

FIGURE 29. CVN Results for 40% Tungsten Alloys. Longitudinal and transverse values averaged.

in Figure 9. At the same time, the rolling performance of the SS-sintered billets improved (i.e., higher reductions were possible without encountering edge cracking). Also, the LP-sintered material loses ductility during rolling due to the change in W particle shape and effective increase in contiguity; the ductility values achieved for rolled and annealed sheet were roughly half those reported by Lux et al. (1982) and by O'Neil and Salyer (1964) for 90% and 85% W, respectively. Based on this reasoning, the most ductile sheet material would be produced from LP-sintered billets with a minimal amount of rolling--only enough to provide the desired thickness and surface finish and to heal any sintering defects that might be present. If SS billet fabrication processes are required to avoid slumping and W particle settling that is encountered in compositions of less than 80% W, a significant amount of rolling and annealing, at the highest practical temperatures, would be required to attain the most ductile material. Certainly, the rolling and annealing schedules used in this study are not optimal, but the properties of the resulting materials indicate what is possible.

Tensile properties of the 40% W sheets with various histories are illustrated in Figure 26. All tensile properties of the sheet rolled from HERF billets are equivalent to those of the SS-sintered sheet, as shown. Annealed properties are: 50 ksi yield strength, 120 ultimate strength, and 55% elongation. Rolling 29% to 40% increases yield strength markedly, to the 140- to 165 ksi range, while ultimate strength increases to 160 to 180 ksi and elongation is reduced to 6% to 9%. Precipitation hardening at 1050°C or 925°C has similar, but milder, effects compared to rolling 29% to 40%; both yield and ultimate strength are increased significantly while ductility is somewhat decreased. Rolling 10% would probably yield the same average tensile properties as precipitation hardening, but with slightly more directionality.

CVN impact energies of the 40% to 90% W are plotted in Figure 27. There is a very rapid increase in toughness as W content decreases (and the proportion of tough matrix increases). Also, the LP-sintered (85% and 90% W) material is significantly tougher than SS-sintered material. Figure 28 shows the relationship between tensile elongation and CVN impact energy for both LP- and SS-sintered material. Although there are only four data points plotted in

Figure 28, the data clearly indicate that for a given slow tensile elongation the SS-sintered material has significantly lower impact toughness than LP-sintered material. Logically, the lower toughness could be related to higher contiguity in the SS-sintered material, since contiguity is a measure of the proportion of weak contacts between the tungsten particles (German, Hanafee, and DiGiallonardo 1984; Churn and German 1984). It is also speculated that LP-sintered material is less strain-rate sensitive because of its lower contiguity and the attending improved stress distribution in the less strain-rate-sensitive matrix.

CVN impact energies of 40% W sheets with different histories are shown in Figure 29. Again, HERF material has the same properties as sintered material. Annealed material has a very high toughness, ~100 ft-lb/in., which reflects the high proportion of tough matrix, about 88 vol%. In contrast, the best toughness for the 90% W material (23 vol% matrix) was 11 ft-lb/in. The 29% and 40% rolled materials maintain high toughness, about 40 ft-lb/in.; combined with the high strength and useful ductility discussed earlier and shown in Figure 26 these are very impressive mechanical properties. The toughness of precipitation-hardened material is also impressive in that it is nearly equal to the toughness of annealed material; at the same time the tensile strength of the precipitation-hardened material is significantly higher (see Figure 26). Therefore, in applications requiring both high strength and toughness, both cold working and precipitation hardening are interesting processing options for 40% W. The applicability of these options to higher W contents should be the subject of future studies.

REFERENCES

Agababova, V. M., and I. N. Chaporova. 1969. "Boundary of the Monophasic γ-Solid Solution Region in the Ternary System W-Ni-Fe." Soviet Power Metallurgy and Metal Ceramics 79:571-576.

Bukatov, V. G., V. M. Romashov, and Y. V. Gostev. 1983. "Effect of Heat Treatment on the Distribution of Elements in the Phase Components of a W-Ni-Fe Alloy." Soviet Powder Metallurgy and Metal Ceramics 21(10):785-788.

Churn, K. S., and D. N. Yoon. 1979. "Pore Formation and Its Effect on Mechanical Properties in W-Ni-Fe Heavy Alloy." Powder Metallurgy 22(4):175-178.

Churn, K. S., and R. M. German. 1984. "Fracture Behavior of W-Ni-Fe Heavy Alloys." Metallurgical Transactions A 15A:331-338.

Dieter, G. E. 1961. Mechanical Metallurgy, McGraw-Hill, New York.

Dzykovich, I. Ya., et al. 1965. "Distribution of Elements During the Formation of Sintered Alloys of the System W-Ni-Fe." Soviet Powder Metallurgy and Metal Ceramics 8(32):655-660.

German, R. M., J. E. Hanafee, and S. L. DiGiallonardo. 1984. "Toughness Variation with Test Temperature and Cooling Rate for Liquid Phase Sintered W-3.5Ni-1.5Fe." Metallurigcal Transactions A 15A:121-128.

Green, E. C., D. J. Jones, and W. R. Pitkin. 1956. "Developments in High Density Alloys." Special Report No. 58, Symposium on Powder Metallurgy, The Iron and Steel Institute, pp. 253-256.

Guy, A. G. 1959. Elements Physical Metallurgy, Addison-Wesley Publishing Co., Inc., Reading, Massachusetts.

Henig, E. T., H. Hofmann, and G. Petzow. 1981. "The Constitution of W-Fe-Ni Heavy Metal Alloys and Its Influence on the Mechanical Properties." Proceedings, 10th Plansee Seminar, Vol. 2, Metallwerk Plansee, Reutte, Austria, pp. 3-35.

Kershaw, J. P. 1964. Ductile Metallic Composites. Dissertation, Massachusetts Institute of Technology, Cambridge, Massachusetts.

Krock, R. H., and L. A. Shepard. 1963. "Mechanical Behavior of the Two-Phase Composite, Tunsten-Nickel-Iron." Trans. Met. Soc. AIME 227:1127-1134.

Lea, C., B. C. Muddle, and D. V. Edmonds. 1983. "Segregation to Interphase Boundaries in Liquid-Phase Sintered Tungsten Alloys." Metallurgical Transactions A 14A:667-677.

Lux, B., et al. 1982. Influence of Impurities in Tungsten and Matrix Composition on the Tungsten-Matrix Interfacial Properties of Heavy Metal Alloys. AD-A129652, National Technical Information Service, Springfield, Virginia.

Minakova, R. V., et al. 1980. "Some Structural Characteristics of the Binder Phase of W-Ni-Fe Alloys." Soviet Powder Metallurgy and Metal Ceramics 19(12):842-846.

Muddle, B. C., and D. V. Edmonds. 1983. "Interfacial Segregation and Embrittlement in Liquid Phase Sintered Tungsten Alloys." Metal Science 17:209-218.

Myhre, T. C. 1979. Process Description for Cold Worked 90 Percent Tungsten Alloy Rods. Y/PG-2275, Oak Ridge National Laboratory, Oak Ridge, Tennessee.

Myhre, T. C. 1980. Effects of Swaging and Aging on Mechanical Properties of Tungsten, Seven Percent Nickel, Three Percent Iron Alloys. Y/PS-40, Union Carbide Corporation, Oak Ridge, Tennessee.

Northcutt, W. G., Jr. 1975. Fabrication Development of Tungsten Alloy Penetrators. Y-1994, Oak Ridge National Laboratory, Oak Ridge, Tennessee.

O'Neil, J. W., and P. N. Salyer. 1964. Effect of Tungsten Composition on the Mechanical Properties of the W-Ni-Fe Heavy Alloy. AD-441038, National Technical Information Service, Springfield, Virginia.

Penrice, T. W. 1980. "Developments in Materials for Use as Kinetic Energy Penetrators." Powder Metallurgy in Defense Technology, Vol. 5, pp. 11-12, Metal Powder Industries Federation, Princeton, New Jersey.

Pfeiler, W. A., and T. C. Myhre. 1980. Investigation of Liquid Phase Sintering Phenomena in Tungsten Base Heavy Alloys. Y/PS-76. Oak Ridge National Laboratory, Oak Ridge, Tennessee.

Stephens, J. R., et al. 1964. Strain Aging Effects in Tungsten Due to Carbon. NASA-TM-X-52000, National Technical Information Service, Springfield, Virginia.

Takeuchi, H. 1967. "Ductility and Matrix Constitution of Sintered W-Ni-Fe Alloys." J. Jpn. Inst. Met., 31(9):1064-1070. [Translation available: ORNL-TR-445, Oak Ridge National Laboratory, Oak Ridge, Tennessee.]

Wehr, A. G. 1962. An Investigation of the Physical Properties of a Sintered Tungsten-Nickel-Iron Alloy. Dissertation, University of Missouri, University Microfilms, Inc., Ann Arbor, Michigan.

Winkler, K., and R. Vogel. 1932. "The Phase Diagram Iron-Nickel Tungsten." Arch F. D. Eisenhuttenwesen 6:165-172.

Yodogawa, M. 1982. "Effects of Cold Rolling and Annealing on the Mechanical Properties of 90W-7Ni-3Fe Heavy Alloys." In Sintering-Theory and Practice, ed. D. Kolar, S. Pejovnik, and M. M. Ristic, Elsevier Scientific Publishing Company, Amsterdam, pp. 519-525.

Zukas, E. G. 1976. "Coating W Composites for Improved Low Temperature Ductility." Metall. Trans. B 7B(1):49-54.

APPENDIX A

DIRECT SINTERING OF THIN SHEETS

APPENDIX A

DIRECT SINTERING OF THIN SHEETS

Heavy metal sheets have been produced in recent years on a commercial basis by Teledyne Firth Sterling, LaVergne, Tennessee. Because of the limited market, heavy metal sheet is produced by rather conventional processes. A relatively thick (about 0.5 in.) billet is rolled to final sheet thicknesses of 0.03 to 0.14 in. Since only about 30% reduction in thickness can be taken between anneals without risking severe cracking, some 4 to 8 rolling sessions and anneals are required to produce finished sheet. It is well recognized that this process is appropriate for the existing market, but it is expensive. If the market for heavy metal sheet is to become substantially larger, production costs will have to be lowered by developing and using processes that reduce or eliminate rolling and intermediate annealing. A minor amount of rolling may improve the mechanical properties of as-sintered material, and thus be desirable for some applications. The object of this work was to explore methods that might be suitable for producing thinner (~ 0.12 in.) sintered billets and to attempt to demonstrate these methods.

Dube (1981) has reviewed particle technology methods for making metal strip:

> "In principle, they essentially consist of making much thinner starting strip than is possible in the conventional way, by a variety of methods such as powder rolling, spray deposition of liquid metal, slurry deposition, reduction of superconcentrate strip, etc. The strip is porous and has relatively poor mechanical properties. It is subsequently densified by a combination of sintering, hot and cold rolling to produce finished strip. It has been shown that the properties of strip produced by these methods are similar to those of conventionally produced strip. The total amount of mechanical working required to produce the finished strip by these methods is rather small. It is possible to produce metal strip from an economically viable small plant based on these methods."

The methods covered by Dube are:

- cold powder rolling
- hot powder rolling
- bonded powder rolling--a metal-binder slurry is cast on a substrate followed by drying and roll compaction
- large particle rolling--rice-grain-sized particles.
- spraying molten metal droplets on a substrate followed by rolling.

All of the above methods have been demonstrated on a commercial scale and are suitable for either continuous or noncontinuous sheet production. We chose to work on methods on a noncontinuous, one sheet at a time basis because this was most easily accomplished with equipment currently available in our laboratory and in heavy metal production facilities. Also, all of the processes reviewed by Dube use rolling to consolidate the powders/particles before sintering. Rolling of powders is a complex task requiring long development time for each application. Powders need to be rolled to high density so that they have sufficient strength to be coiled, bent around corners, transported through the sintering furnace, etc. High density may hinder the deoxidizing process that takes place during sintering and that is necessary to develop good ductility and toughness in tungsten heavy metals. Unfortunately, our work focuses on green billets of about 0.12 in. in thickness, a rather stiff section not tolerant of bending and coiling. Also, our work has shown that very low-density green billets can be sintered to high density. For these reasons, our work was concentrated on methods that might be suitable for producing unusually thin as-sintered billets on the order of 0.1 in. thick. These sintered billets might be used directly or rolled to some extent to improve mechanical properties, finish, thickness uniformity, etc., if required by the application. The following methods selected for further study are based, at least partially, on our experience with tamped, dry powder beds, which was described earlier in this report:

- binderless dry powder
- conventional binders
- cold plastics

- thermoplastics or thermosets
- slurry casting.

A generalized process flow sheet for all the thin billet fabrication methods is shown in Figure A.1. All of the selected methods require low forming pressures, thus obviating the need for large-capacity presses. For instance, a sintered billet 20 in. by 30 in. would be about 26 in. by 38 in. in the green, as-pressed state, an area of nearly 1000 in.^{2} Conventional pressing pressures are 10 to 20 tons per square inch, which translates into a hydraulic press capacity of 10,000 to 20,000 tons. Alternatively, billets of this size would require an isostatic press at least 3 ft in diameter.

All the above methods except those using thermoplastics or thermosets produce weak, fragile billets that must be presintered in the mold in which they were formed. The presinter is then strong enough to be resettered for sintering. Presintering can be accomplished at reduced temperatures to minimize dimensional variations caused by mold distortion and to allow a wider variety of mold materials to be considered. A few tests were run to establish approximate presinter temperatures and to furnish a guide for mold material selection.

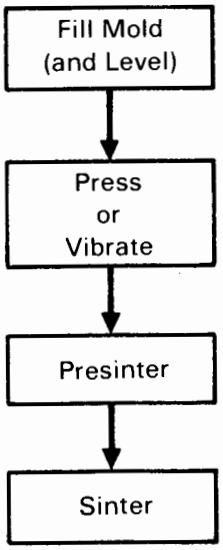

FIGURE A.1. Generalized Process Flow for Thin Billet Fabrication. Individual methods vary in the first two steps. Presinter and sinter are common to all.

Presintering 90% W for 2 h at 1100°C resulted in virtually no sintering shrinkage, but the billet had sufficient strength to be handled without great care. Billets of 40% W presintered at 900°C. Some possible mold materials are alumina, zirconia, quartz, molybdenum, tungsten, graphite, and superalloys. All of these materials were tried. Only alumina or zirconia can be used without coatings; the rest stuck or reacted with the powder. Molybdenum plate coated with alumina by the Rokide® flame spray process worked very well. Coating adherence was very good even when cycled to 1400°C.

Presintered billets need to be resettered for sintering in a manner that allows the billet to shrink during sintering without cracking. Very smooth settering plate, loose settering powder, and tilting the settering plate are conventional possibilities. Gas levitation has been used in continuous production of stainless steel strip (Sturgeon and King 1982). In any event, this is no trivial problem, and it becomes more important as the billet area grows and the thickness decreases. In this study, green billets of up to 8 in. by 18 in. by 3/16 in. thick were sintered without cracking if proper precautions were taken. In fact, anything crack-free after bakeout was crack-free after both presinter and sinter. It was found that LP sintering could heal some rather large cracks; SS sintering always retained cracks and all other features present before sintering.

Each of the thin billet fabrication methods tried in this work is discussed separately in the following subsections. Because no method was completely developed and proven successful, the discussions are brief. The general method, problems encountered, and promise for future development are addressed.

BINDERLESS, DRY POWDER METHOD

The dry powder method illustrated in Figure A.2 is essentially the same as the method used to make small, thick billets (3.5 in. by 0.5 in.) for this study. Good, crack-free billets were produced with a success rate of 70%. Large-area, thin billets are much more difficult to produce by this method.

® Registered trademark of the Norton Company.

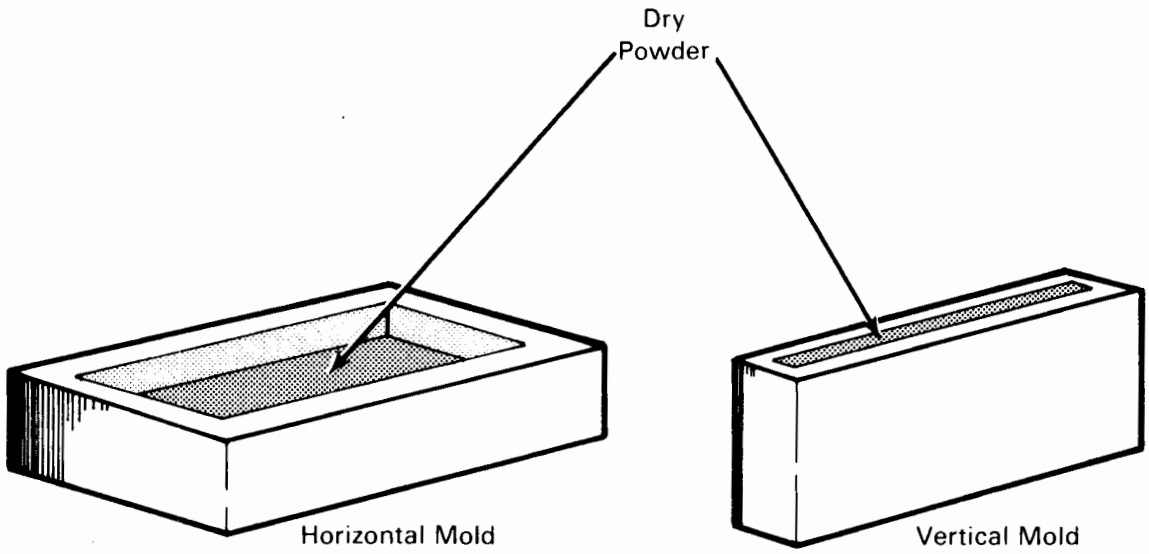

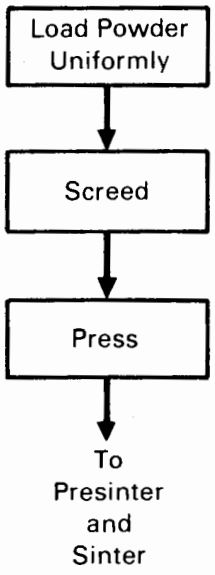

FIGURE A.2. Binderless, Dry Powder Method

The molds must be dimensionally accurate and unwarped. The powder has to be laid into the mold in a very uniform manner (i.e., with very uniform density), otherwise differential sintering shrinkage will crack the billet. Mechanical vibration can aid in obtaining this uniform fill density, but mechanical forces can also introduce nonuniformities and cracks in seemingly mysterious ways, as we discovered. The screeding has to be done in order to obtain a uniform thickness in horizontally loaded billets. However, the screeding action packs the powder ahead of the screed. This is no real problem with the vertical mold, but loading the powder uniformly into the thin, deep slot is a problem. Density of the as-loaded powder is only about 25%; in that state the powder mass is very weak and extremely susceptible to cracking due to mechanical stresses and to sintering shrinkage. Pressing the powder at just a few psi will increase green density and strength, but the mold must be rigid and flat. Otherwise, the mold flexure during pressing will cause cracks. The higher the pressing pressure, the more important it is that the mold be rigid and flat. Since the mold must go through presintering, warpage can occur; very stable mold material is required.

We had little success with this technique in producing large-area, thin billets. Greater success was obtained with the techniques that follow; they all use binders. However, we were able to produce a couple of 1-in.-diameter rods by loading dry powder vertically into alumina tubes and sintering in the horizontal position, which gives some hope for this binderless method. It must also be remembered that LP sintering heals all but the largest cracks.

CONVENTIONAL BINDERS

The process and all the comments regarding the binderless, dry powder method still apply when binders are added to the powder. Two necessary process steps are added: 1) blending in the binder and 2) baking out the binder (usually part of the presinter cycle). The binder could be a wax, a soap, an oil, or even water. About 0.5% to 2% by weight is the usual amount used in high-pressure pressing; somewhat more would be required to develop good green strength in low-pressure pressings. The binder can improve interparticle flow

and thus increase green density slightly. The principal benefit of the binder is that it increases green strength, which means improved resistance to cracking caused by vibrations or mold flexing.

We have successfully made a billet 5.4 in. by 10.6 in. by 0.17 in. thick using 4% water as a binder. The water was added to the powder through the intensifier bar of a Liquid-Solids® twin-shell blender. The resulting powder had extremely poor flow characteristics; it was run through a 5-mesh sieve and dropped directly into a horizontal mold through a large funnel in such a way that very little material had to be moved to complete the screeding job. After pressing at 1000 psi, the top punch was removed and the compact was dried at 125°C for two hours and then sintered to a final density of 98.2% of 14.0 g/cm^3 (70% W composition). The dried, green compact appeared to be hard and strong, indicating that some bonding occurs through a corrosion reaction between the water and powders. Reduction of the corrosion products, probably hydroxides as well as oxides, will occur during the deoxidization stage of the sintering cycle (Lux, Jangg, and Danninger 1981).

An attempt to make a thicker, 0.5-in.-thick billet resulted in a cracked billet after drying too rapidly on a hot plate; also, the mold had warped in sintering the first plate which may have caused some of the cracking due to mold flexure during pressing. Although this process is more promising than the binderless dry powder approach, it is evident that its success depends on tooling that is geometrically stable after repeated presintering cycles, and on very careful attention to powder preparation, layup, pressing, and bakeout. Any problems identified in our attempts to produce 5.4 in. by 10.6 in. billets will be magnified in attempting larger-area billets. Again, LP sintering would eliminate all but the largest cracks.

COLD PLASTIC METHOD

The cold plastic method outlined in Figure A.3 uses plasticizing additives to make a powder mass that can be worked like clay. Many ceramic and plastics forming processes might be used to form thin, large-area billets. We used 1%

® Registered trademark of the Patterson-Kelley Company.

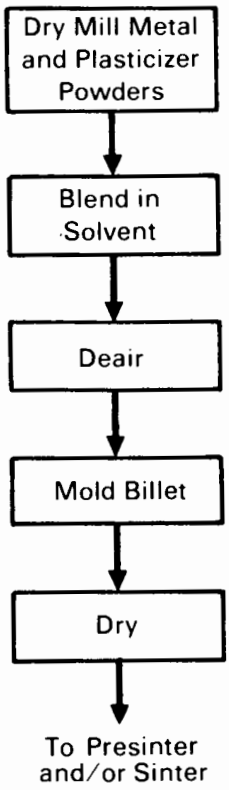

FIGURE A.3. Cold Plastic Method

Klucel H hydroxypropylcellulose, a product of Hercules, Inc., with 4% to 5% water to plasticize the powder mass. The Klucel H, a minus 20-mesh powder, was dispersed in the heavy metal alloy powders by dry ball milling. The water was then blended into the powders by adding it through the intensifier bar of a Liquid-Solids blender. This mix was then aged overnight to allow the solvent to dissolve the Klucel H, which is necessary for the development of plasticity.

To date we have had very little experience with forming these cold plastics in a transfer press. The material extrudes very easily from the transfer chamber into the mold, but it sticks to the mold, and probably has some entrained air pockets. Sticking could be eliminated by drying in the mold, either by heat or vacuum. The air pockets could be kept to minimal size either by deairing the plastic mass before forming or by drying the formed part under pressure in the mold. The advantages of this cold plastic method are: 1) a variety of plastic forming processes are applicable, 2) the plastic mass can flow laterally under uniaxial pressure and thus produce a superior uniformity

of powder density, 3) the plastic mass has some useful elasticity, and 4) when dried the Klucel H adds considerable green strength to the molded powder; this strength may be sufficient to allow the handling needed to setter the molded part for direct sintering (that is, without the presintering step). Many organic solvents, particularly alcohols, can be used if water is found to be unsatisfactory.

THERMOPLASTICS OR THERMOSETS

As the name implies, this method uses thermoplastic or thermoset polymers and elevated temperatures to accomplish forming. Usually, minor amounts of other specific additives are employed for plasticizing, lubricating, stabilizing, etc. The mixed powders and additives are then pelletized to remove air from fine porosity and to produce a suitable feed to the molding machine. Injection molding, compression molding, and extrusion are the major possible molding techniques, as shown in Figure A.4.

A high volume of polymer, on the order of 50%, is required for sufficient flow. The bakeout cycle must therefore be carefully developed to avoid cracking and detrimental residues from the polymer and additives, such as carbon and alkali metals. This method is capable of forming intricate parts in high

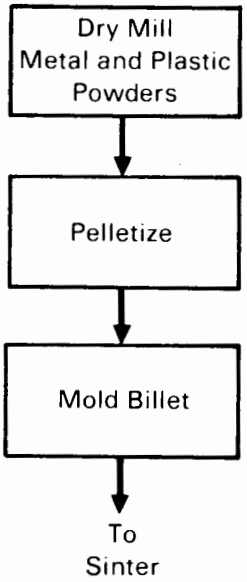

FIGURE A.4. Thermoplastic or Thermoset Methods

volume at low cost. The molded parts would have very good green strength; they could be handled and settered for direct sintering without a separate presintering step.

To date only a few crude trials of this method have been made. It was found that about 6% Klucel H (in 70% W powder) would extrude properly in the transfer molding press. Klucel H is thermoplastic and has a density of about 0.5 g/cm^3. The 6% by weight Klucel H addition is about 60 vol% of the metal powder/Klucel H mixture. Incomplete parts were formed due to insufficient feed material. No bakeout of these incomplete parts was attempted.

SLURRY CASTING

Slurry casting has been practiced on a commercial scale to produce thin, continuous strip (Dube 1981). The method has promise for making the relatively thicker, large-area billets. The method is outlined in Figure A.5. In principle the metal powders are dispersed in a fluid so that the powders will flow by

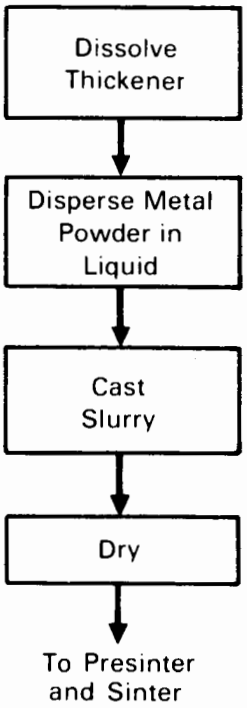

FIGURE A.5. Slurry Casting Method

gravity, like water, to fill a dimensionally accurate, level mold. The mold must be suitable for presintering, and must be durable and dimensionally stable enough to be reused many times. The dense tungsten powders settle so rapidly from suspensions in unmodified fluids that the powder mass loses its fluidity and will not fill the mold. If the fluid is thickened, then adequate suspension of the tungsten powder particles ensures that the slurry will flow well enough to fill the mold. After drying, the green density of slurry castings is about 50%. Success achieved by this method was limited, but was sufficient to demonstrate the potential. Two different thickener fluid systems were tried: 1) Klucel H hydroxypropylcellulose in isopropyl alcohol, and 2) oleic acid in toluene.

Isopropyl alcohol is a borderline solvent for Klucel H. Addition of 10% water made clear solutions. About 0.6% to 0.7% Klucel H in the 90% isopropyl-10% water mixture was sufficient to maintain adequate flow of the slurry into the 8-in. by 8-in. by 0.15-in.-deep graphite molds. Higher Klucel H contents, up to 1% of the fluid weight, were tried, but with increasing incidence and severity of "elephant skinning," a deep wrinkling of the surface of the casting. A rapid air-flow pattern around the casting during drying was found to enhance elephant skinning. At 1% Klucel the slurry was too viscous and would not fill the mold. Good castings could be made using 1 cc of the 0.6% Klucel H solution with 10 g of metal powder (85% W). This is more liquid than required to fill the mold, and a very visible thickness shrinkage occurs. At 11 g of metal powder per cc of liquid the castings invariably cracked upon drying, although the shrinkage was minimal.

Problems encountered with this method were: 1) occasional cracking, 2) thickness variations from end to end, 3) extreme thickness loss around the edge of the mold due to wicking, and 4) low sintered densities (most likely related to the Klucel H, possibly sodium residue). All these problems should be solvable with proper tooling, a better thickener, and more development.

Good castings could also be made with a different liquid system, 1% oleic acid in 7% toluene with 93% metal powder (85% W). Very careful, slow drying is necessary to avoid cracking. Good, normal sintered densities were obtained. When the oleic acid is burned out at 180°C, the residue weakly bonds the powder

casting together, possibly allowing the handling necessary to resetter the casting for direct sintering without a separate presinter step. The burnout operation frequently caused bowing of the casting, resulting in the casting cracking from its own weight. Up to 6% oleic acid mixtures can be troweled and smoothed. There are some interesting possibilities for the oleic acid, or similar, formulations.

REFERENCES

Dube, R. K. 1981. "Particle Technology Methods for Making Metal Strip." Powder Metallurgy International, Vol. 13, No. 4, Vol. 14, Nos. 1-3, and Vol. 15, No. 1.

Sturgeon, G. M., and K. J. King. 1982. "Development of Powder Route for Production of Stainless Steel Strip." Powder Metallurgy, Vol. 25, No. 2, pp. 57-61.

PNL-5218
UC-25

DISTRIBUTION

No. of Copies

OFFSITE

27 DOE Technical Information Center

T. W. Penrice
Teledyne Firth Sterling
#1 Teledyne Place
LaVergne, TN 37086

R. R. Hulbert
Teledyne Firth Sterling
#1 Teledyne Place
LaVergne, TN 37086

J. A. Mullendore
GTE Sylvania
Chemical and Metallurgical Division
Towanda, PA 18848

O. W. Nichols
Kennemetal, Inc.
P.O. Box 346
Latrobe, PA 15650

M. J. Ostermann
Teledyne Wah Chang Huntsville
7300 Highway 20, West
Huntsville, Alabama 35806

S. R. Weigel
GTE Sylvania
Chemical and Metallurgical Division
P.O. Box 2795
Los Angeles, CA 90051

No of Copies

ONSITE

2 DOE Richland Operations

H. E. Ransom

53 Pacific Northwest Laboratory

W. E. Gurwell (35)
G. B. Dudder
R. G. Nelson
N. C. Davis
R. H. Jones
R. S. Kemper
C. R. Hann
E. L. Courtright
P. E. Hart
A. M. Sutey
K. R. Sump
P. L. Whiting
Publishing Coordination (2)
Technical Information (5)